ePIC pfRICH General meeting

High Momentum Particle Identification Detector (HMPID) at the ALICE experiment at LHC

Giacinto de Cataldo[a], Giacomo Volpe[b]

[a]INFN Bari, CERN
[b]University & INFN, Bari

19/10/2023

ALICE goal

ALICE is designed to study the physics of strongly interacting matter under extremely high temperature and energy densities to investigate the properties of the quark-gluon plasma.

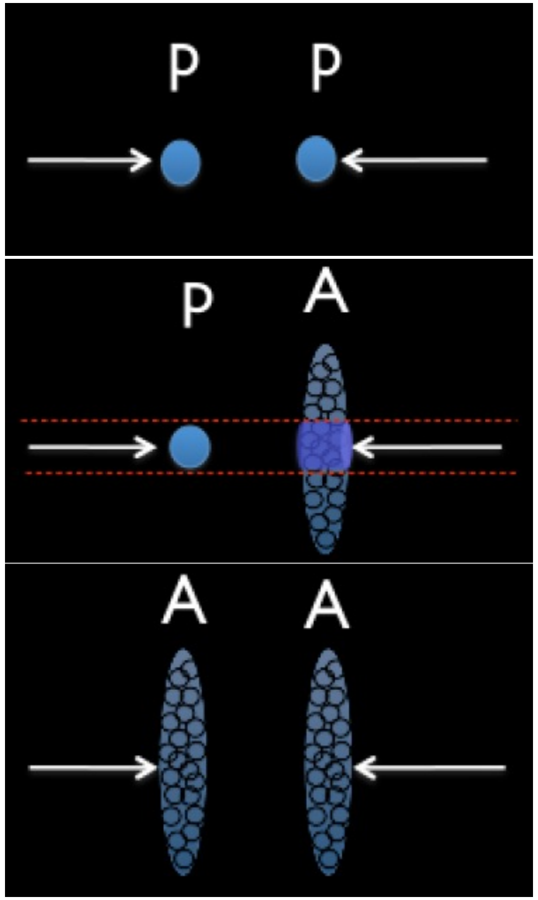

- Proton-proton collisions:
  - high energy QCD reference.
  - collected pp data at $\sqrt{s}$ = 0.9 TeV, 2.76 TeV, 7 TeV, 8 TeV, 13 TeV (2009, 2010, 2011, 2012, 2016,2016)

- proton-nucleus collisions:
  - initial state/cold nuclear matter.
  - collected p-Pb data at $\sqrt{s_{NN}}$ = 5.02 TeV (2012, 2013)

- nucleus-nucleus collisions:
  - quark-gluon plasma formation!
  - collected Pb-Pb data at $\sqrt{s_{NN}}$ = 2.76 TeV, 5.02 TeV (2010, 2011, 2015)

ALICE must measure the yields of produced charged pions, kaons and protons in a wide momentum range and in several colliding systems.

ALICE apparatus

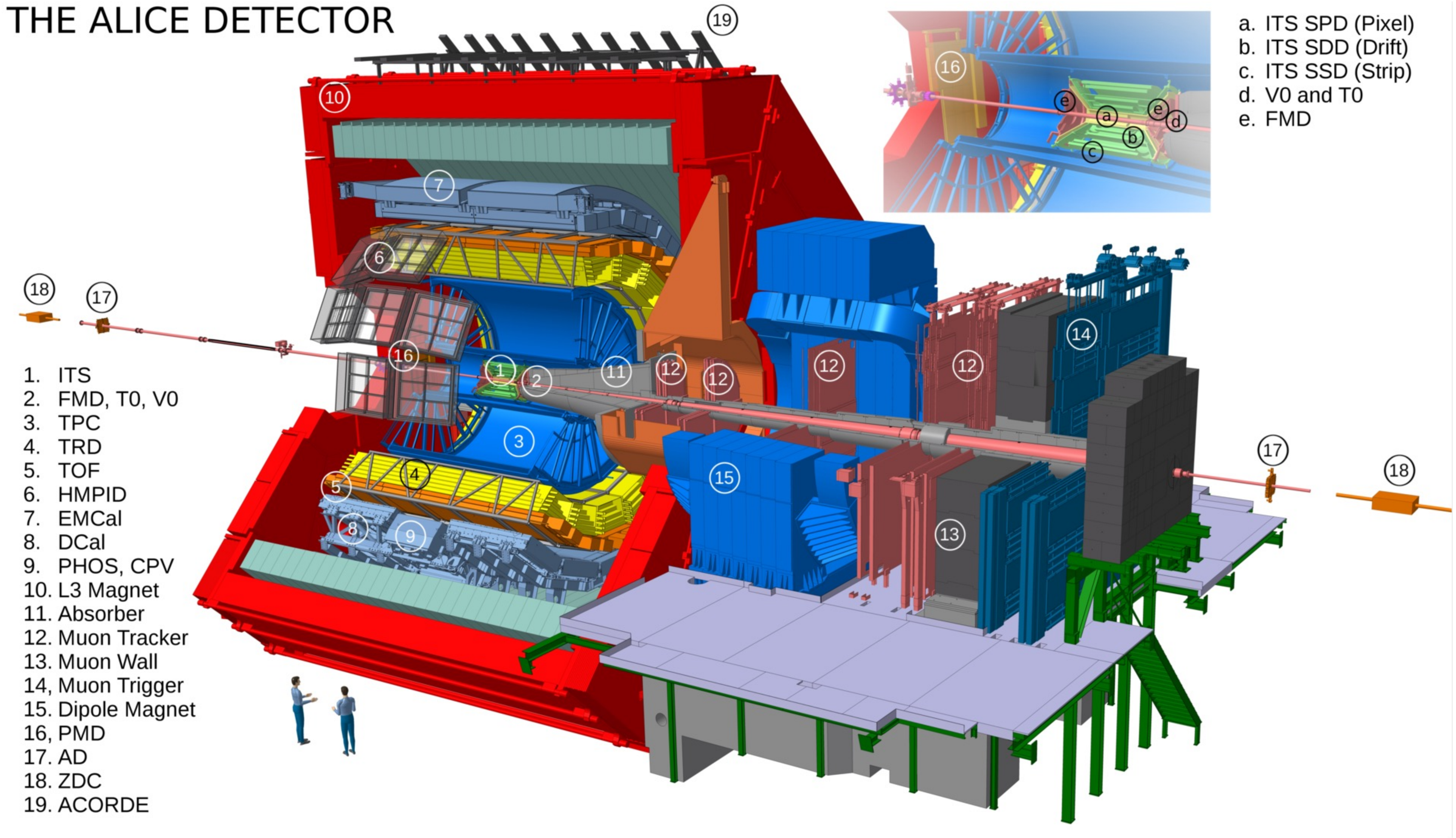

ALICE apparatus

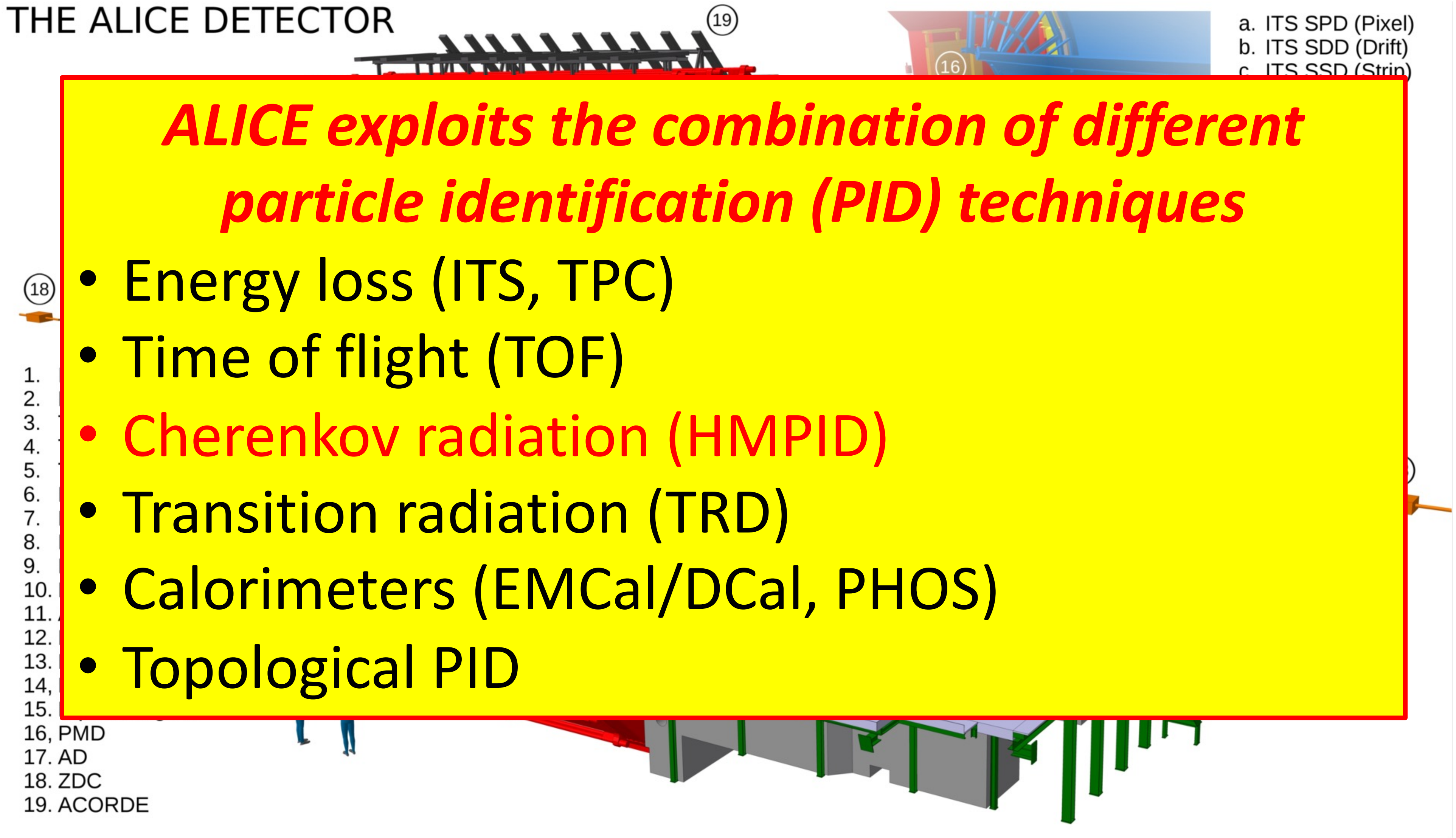

ALICE exploits the combination of different particle identification (PID) techniques

- Energy loss (ITS, TPC)
- Time of flight (TOF)
- Cherenkov radiation (HMPID)
- Transition radiation (TRD)
- Calorimeters (EMCal/DCal, PHOS)
- Topological PID

Particle Identification in ALICE: momentum ranges

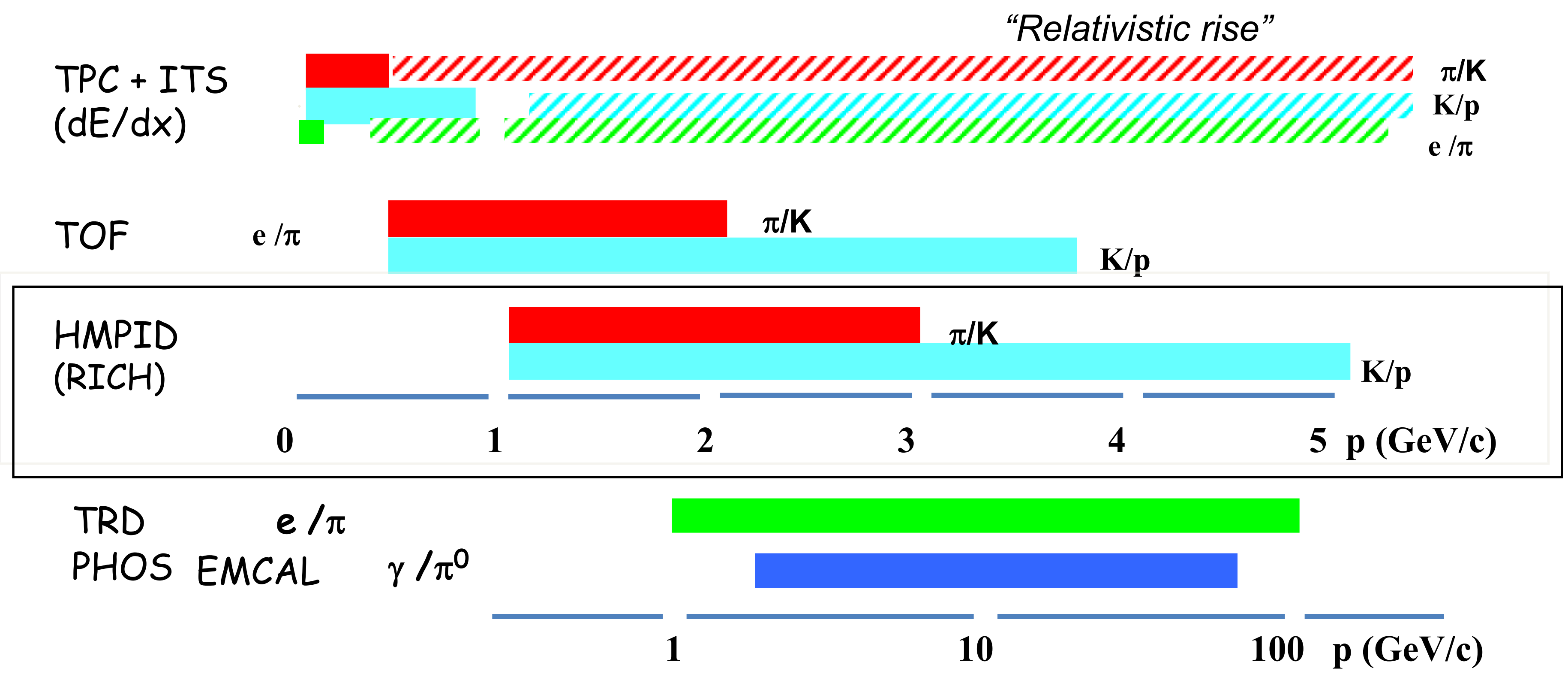

Solid: track-by-track

Dashed: only statistical

HMPID description

- The ALICE-HMPID (**H**igh **M**omentum **P**article **I**dentification **D**etector) performs charged particle track-by-track identification by means of the measurement of the emission angle of Cherenkov radiation and of the momentum information provided by the tracking devices.

- It consists of seven identical proximity focusing RICH counters.

RADIATOR
15 mm liquid C_6F_{14},
n ~ 1.2989 @ 175nm, β_{th} = 0.77

PHOTON CONVERTER
Reflective layer of CsI
QE ~ 25% @ 175 nm.
The largest scale (11 m²) application of CsI photo-cathodes in HEP
≈ 5 % of TPC acceptance

PHOTOEL. DETECTOR
- MWPC with CH_4 at atmospheric pressure (4 mm gap) HV = 2050 V.

- Analogue pad readout

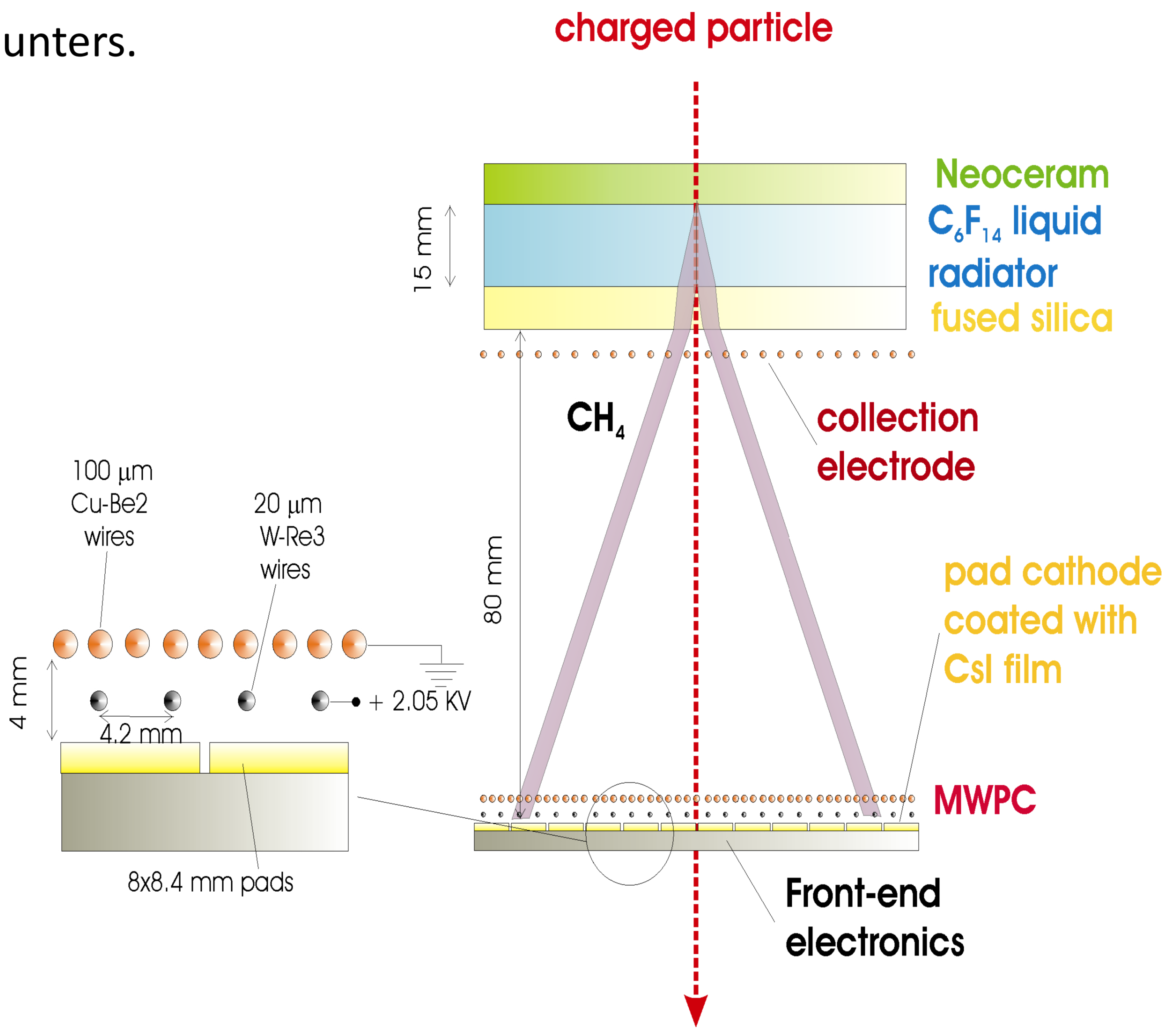

HMPID is installed in the ALICE magnet since September 2006

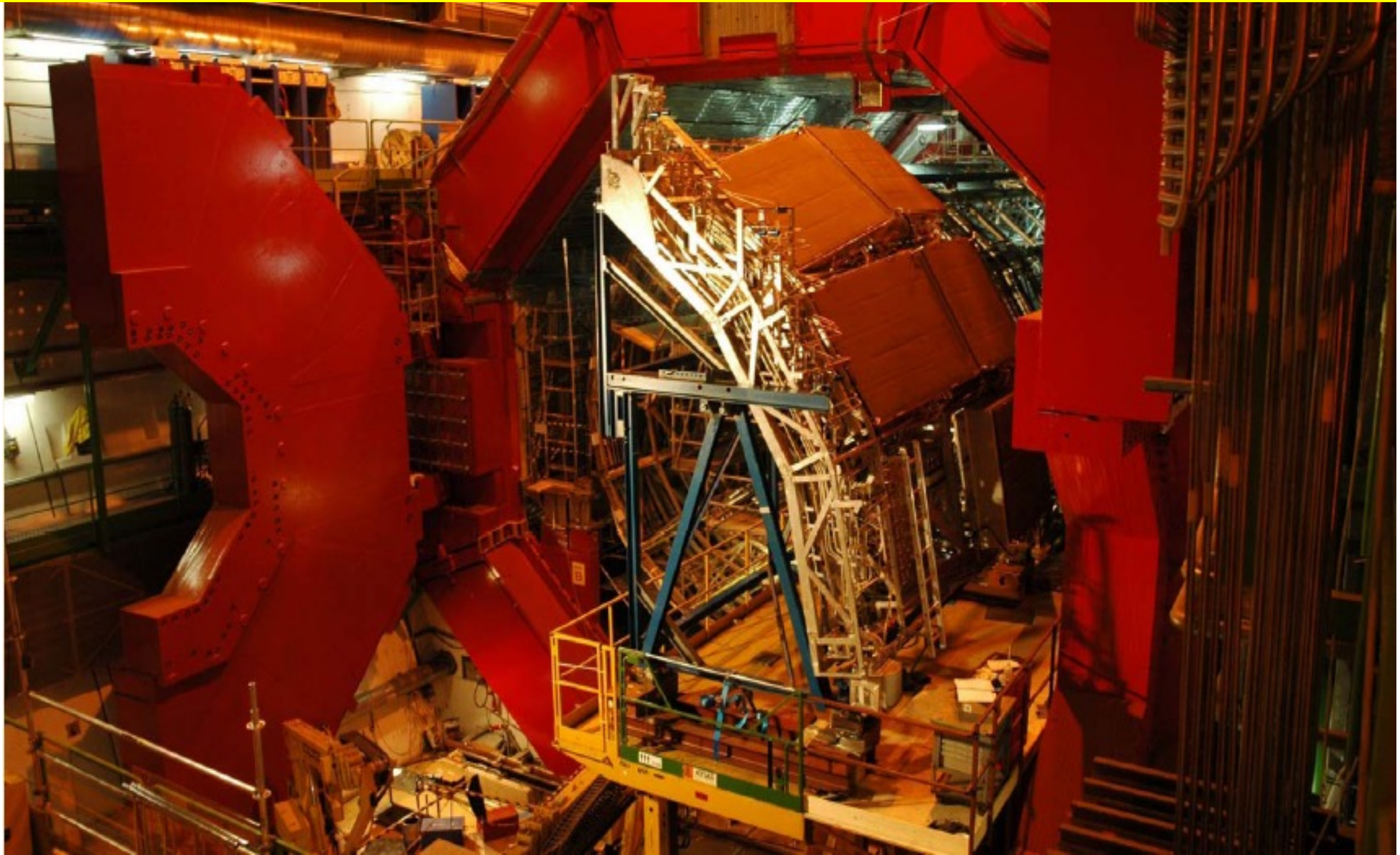

HMPID detector description

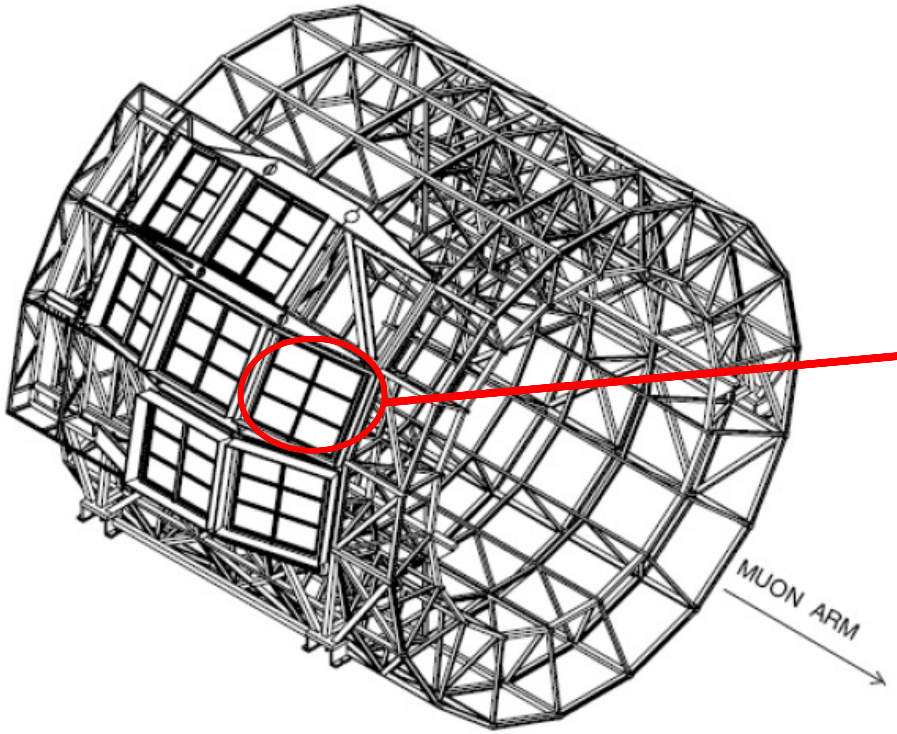

Six photo-cathodes per module

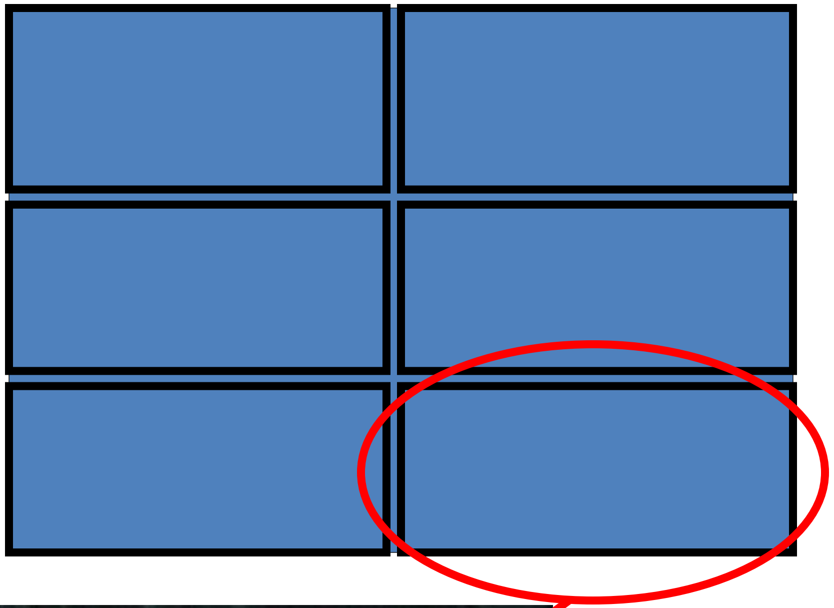

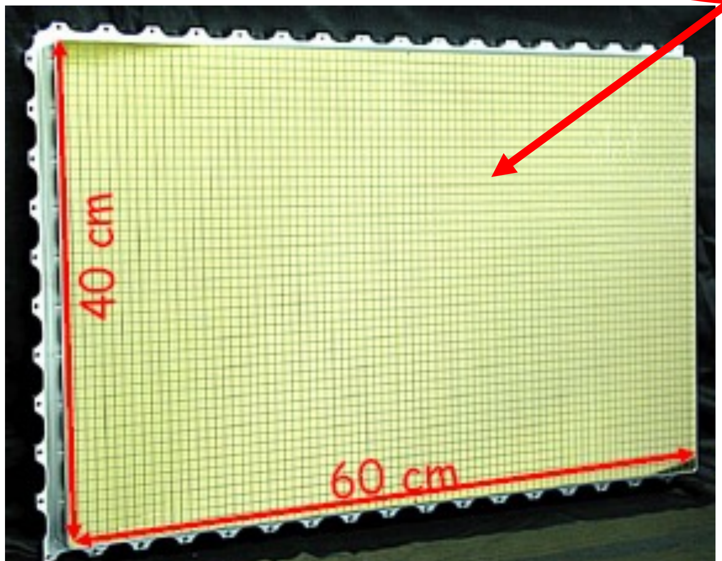

CsI photo-cathode is segmented in 0.8x0.84 cm pads

HMPID detector description

- FEE and RO electronics is based on GASSIPLEX and DILOGIC chips developed within the HMPID project

- GASSIPLEX: 16-channel analogue multiplexed low-noise signal processor, the noise level is 1000 e^-, dead/noisy pads are less than 200 out of 161280

- DILOGIC: individual threshold and pedestal setup

- 42 photo-cathodes are segmented into 3840 pads with individual analog readout.

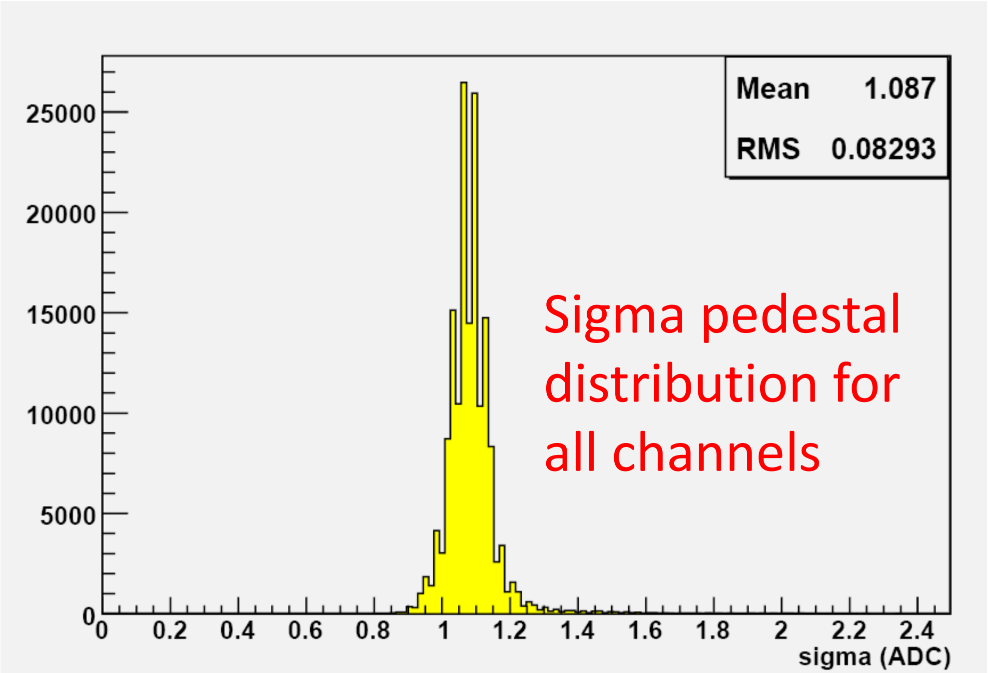

GASSIPLEX DILOGIC

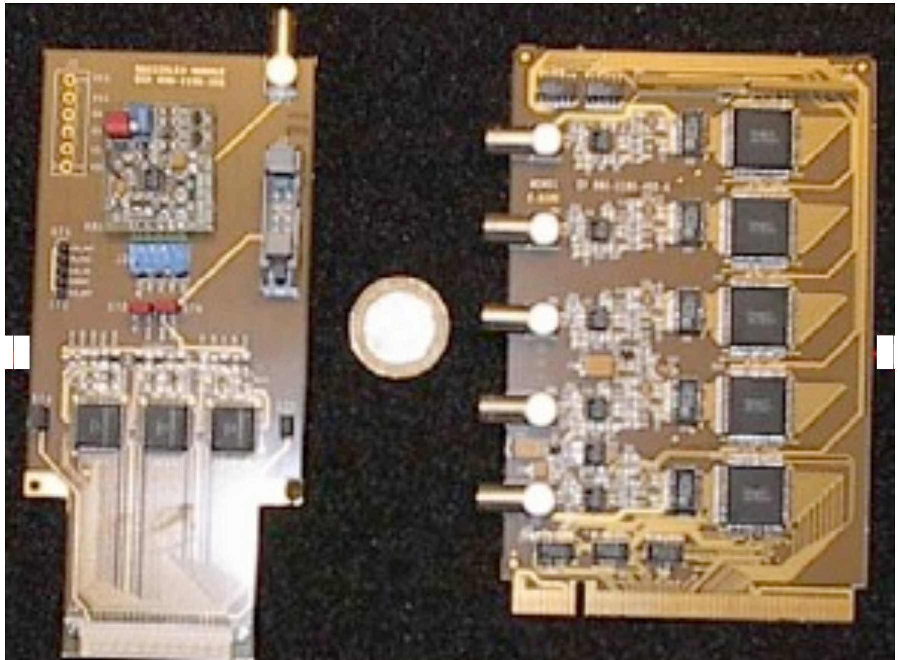

The Detector Control System

- Detector Control System (DCS) developed in the PVSS SCADA provided a full detector monitoring, archiving of condition data and remote operation.
- The user interface (UI) of the HMPID DCS . The command execution is based on a Finite State Machine (FSM).

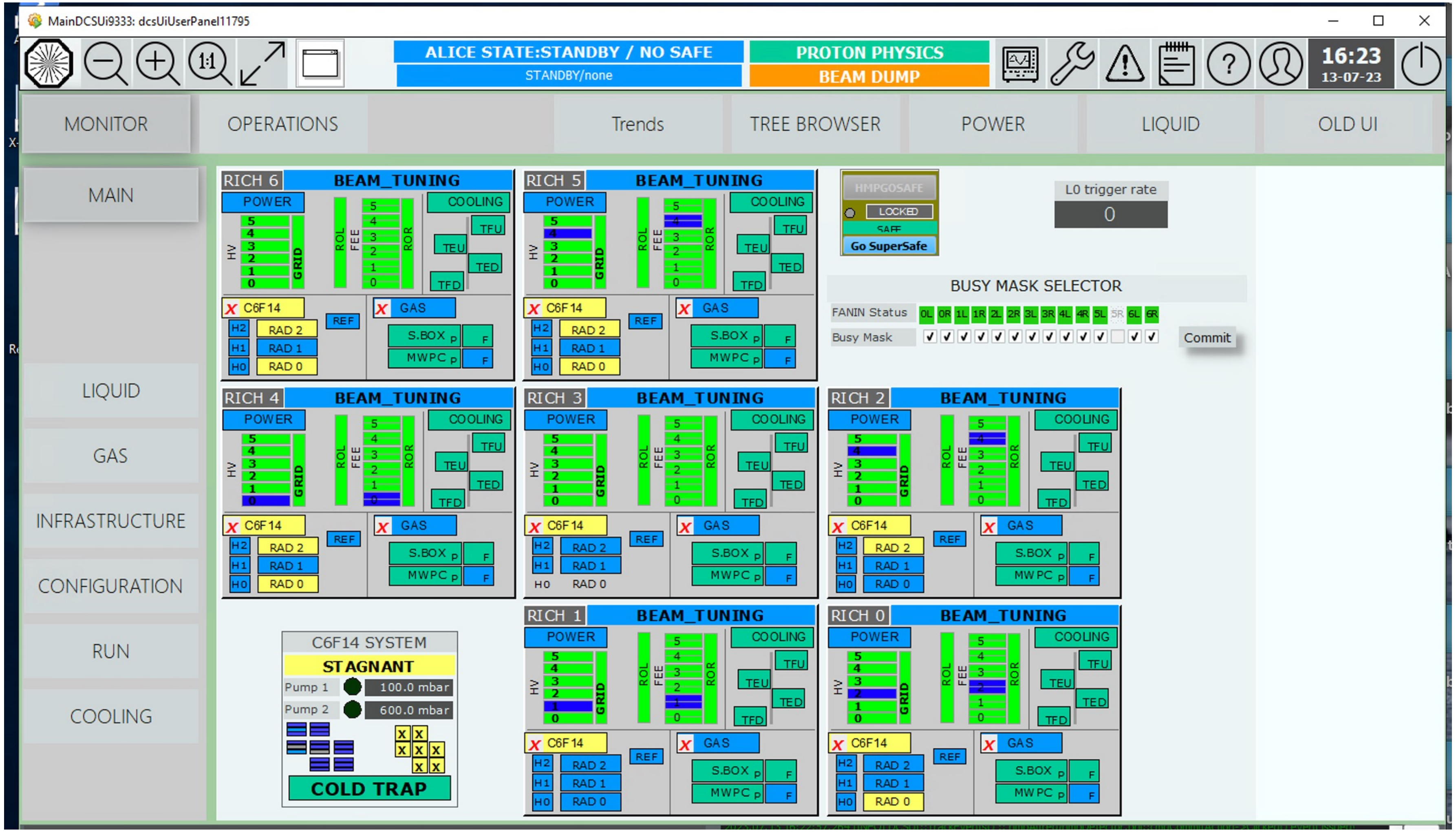

Sub-system segmentation in one RICH module

- 6 CsI pad Photocathodes (PC's);
- 6 x HV sector of 48 anodic wires (HV's);
- 6 x FEE sectors (FEE's);
- 2 RO sectors (ROR-L)
- Details : CERN/LHCC 98-19 ALICE TDR 1 14 of August 1998.

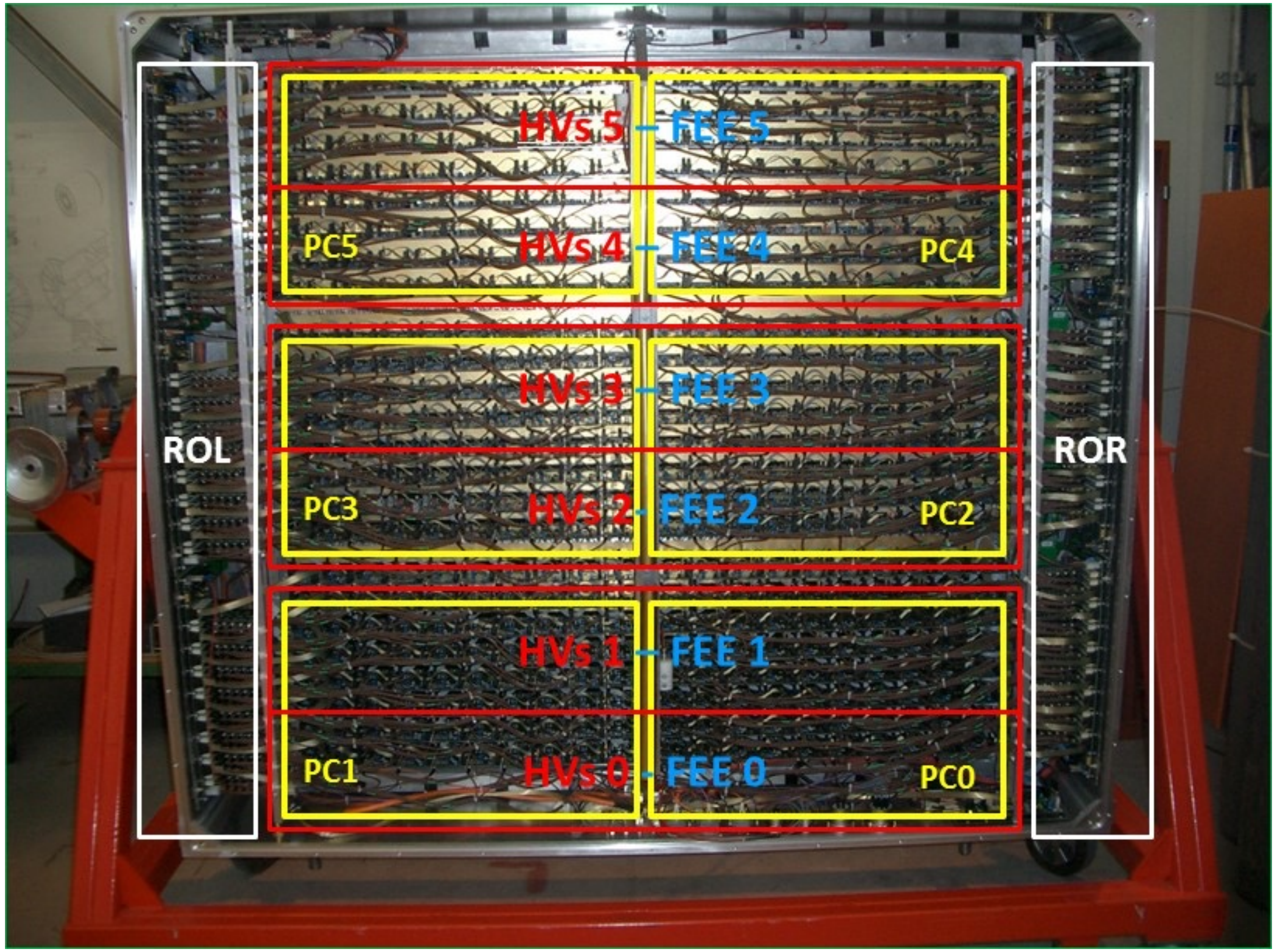

C_6F_{14} circulation and purifying systems

- Safe C_6F_{14} circulation by gravity flow;
- Stable transparency to Č photons;
- Separated control for each radiator vessel;
- C_6F_{14} : 3M PF5060DL.

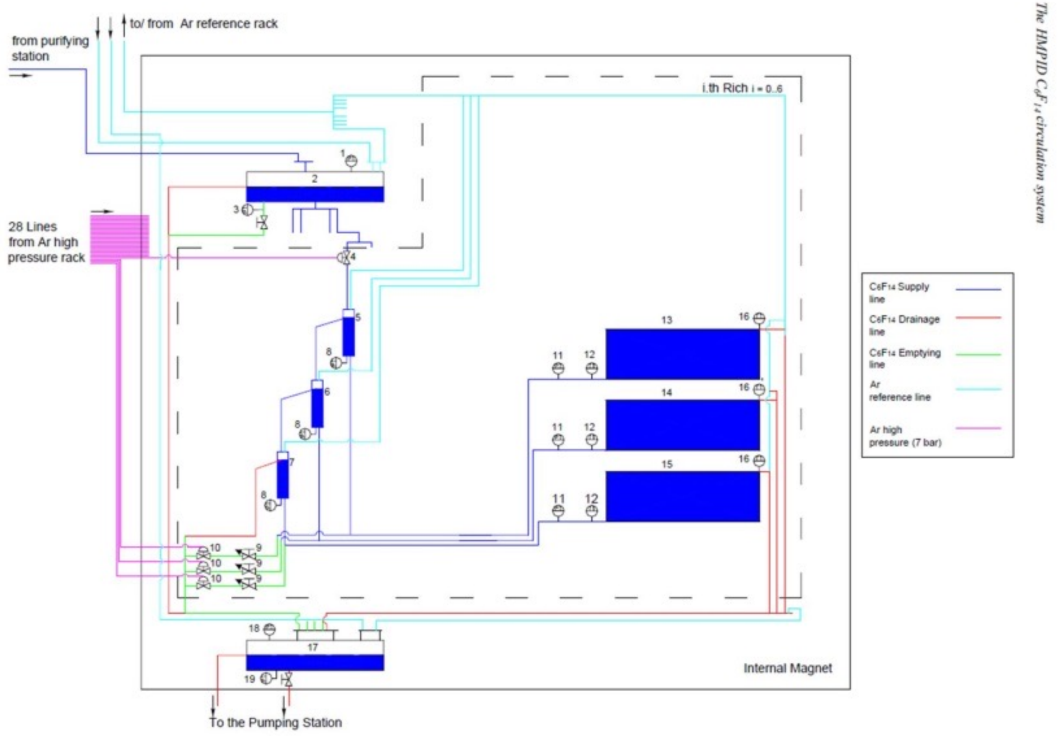

Fig 10 Schematic of the distribution station for one module.

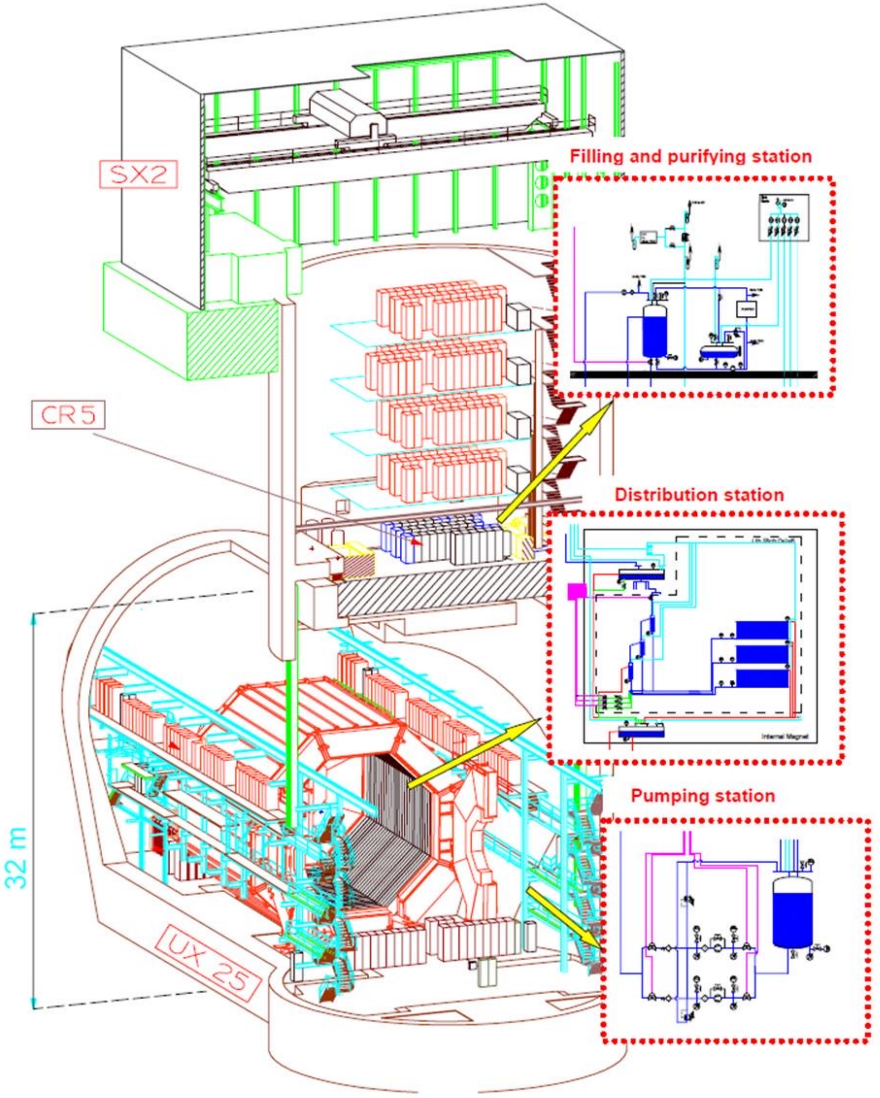

Fig. 6 Location of the three units of the HMPID liquid system in the experimental cavern.

C_6F_{14} Transparency monitoring

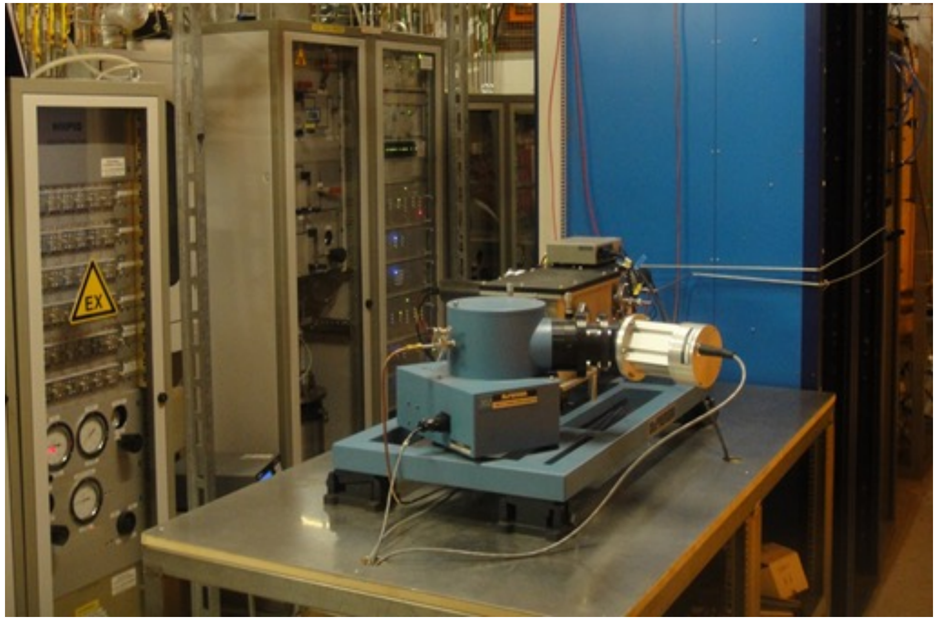

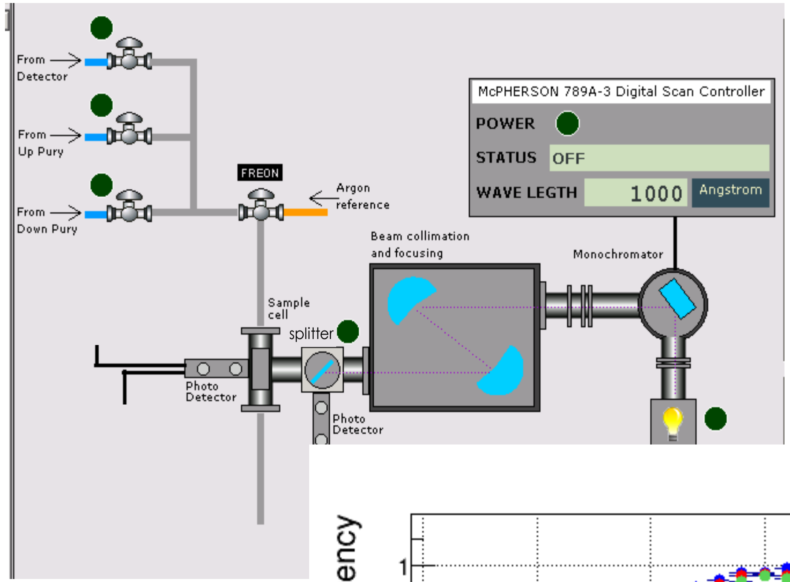

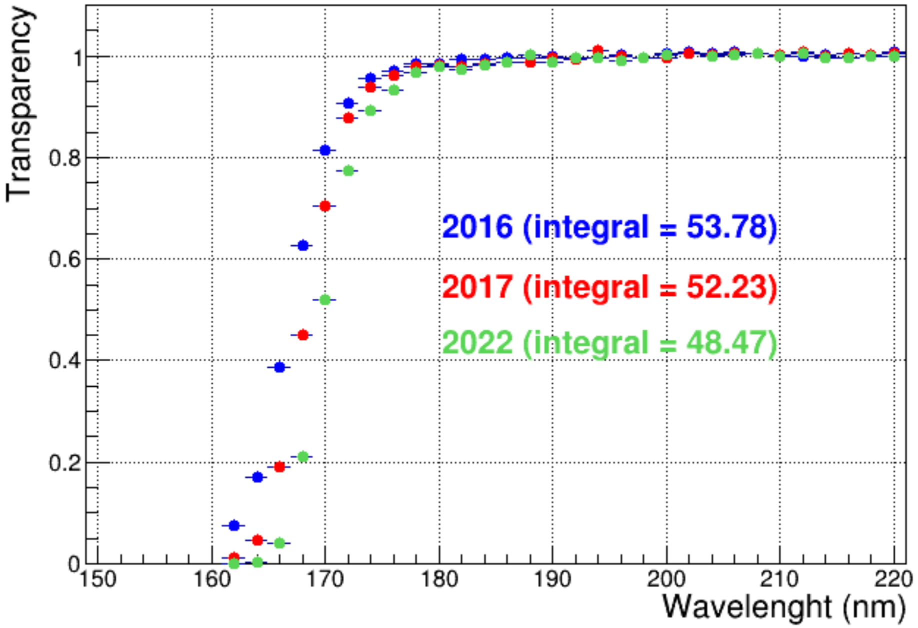

Detector stability: MWPCs gain

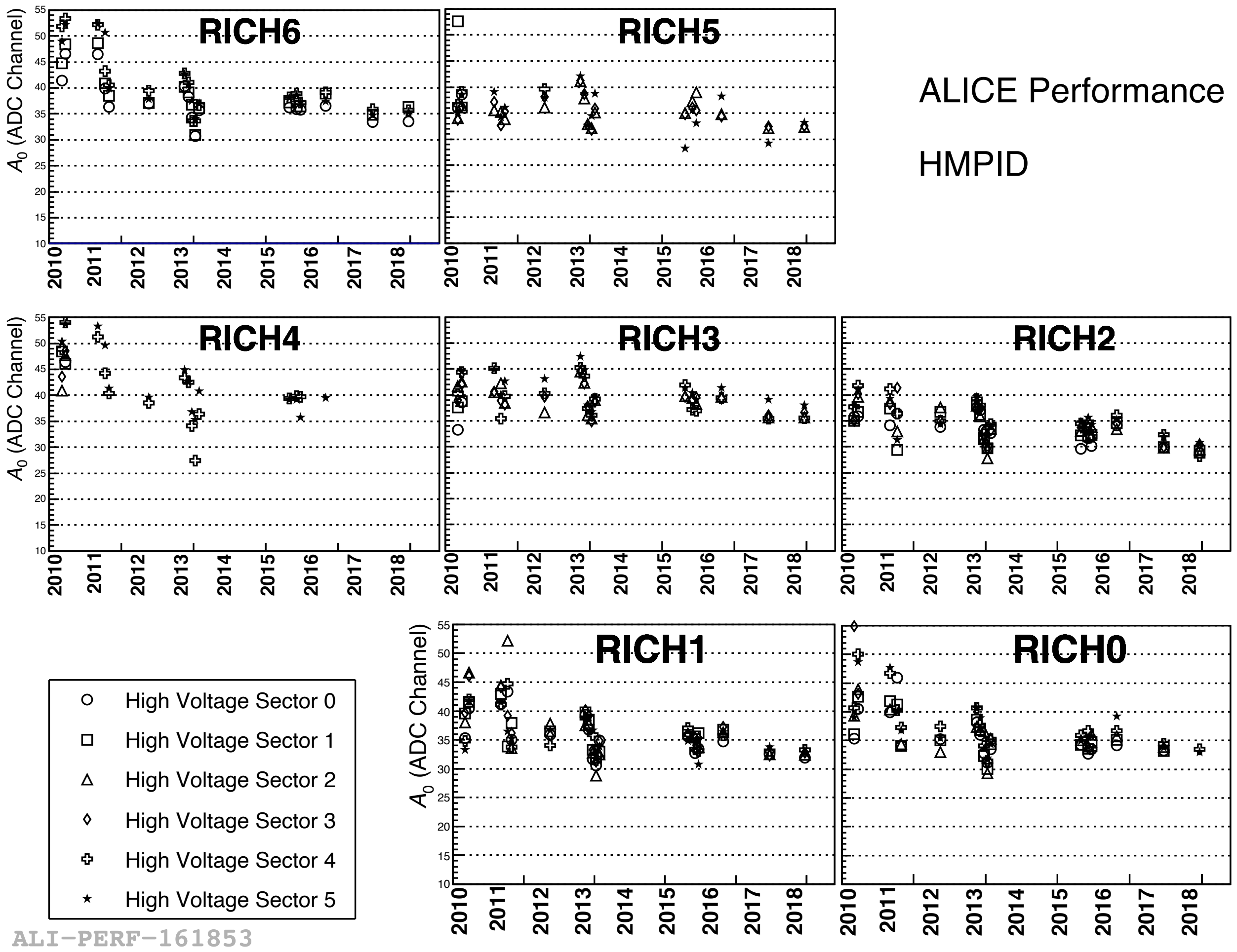

ALICE Performance

HMPID

Photo-electron pulse height distribution

$$P(A) = \frac{1}{A_0} e^{-A/A_0}$$

- HV equalization (Sept. 2011) to set $A_0 \approx 35$;
- Gain variations ≈ ± 15%;
- A reduction of 20% on A_0 -> photoelectron detection efficiency loss of 3% ($A_{th}/A_0 \approx 4/35$) . No effects on the PID performance!

Detector stability: number of detected ph.e.

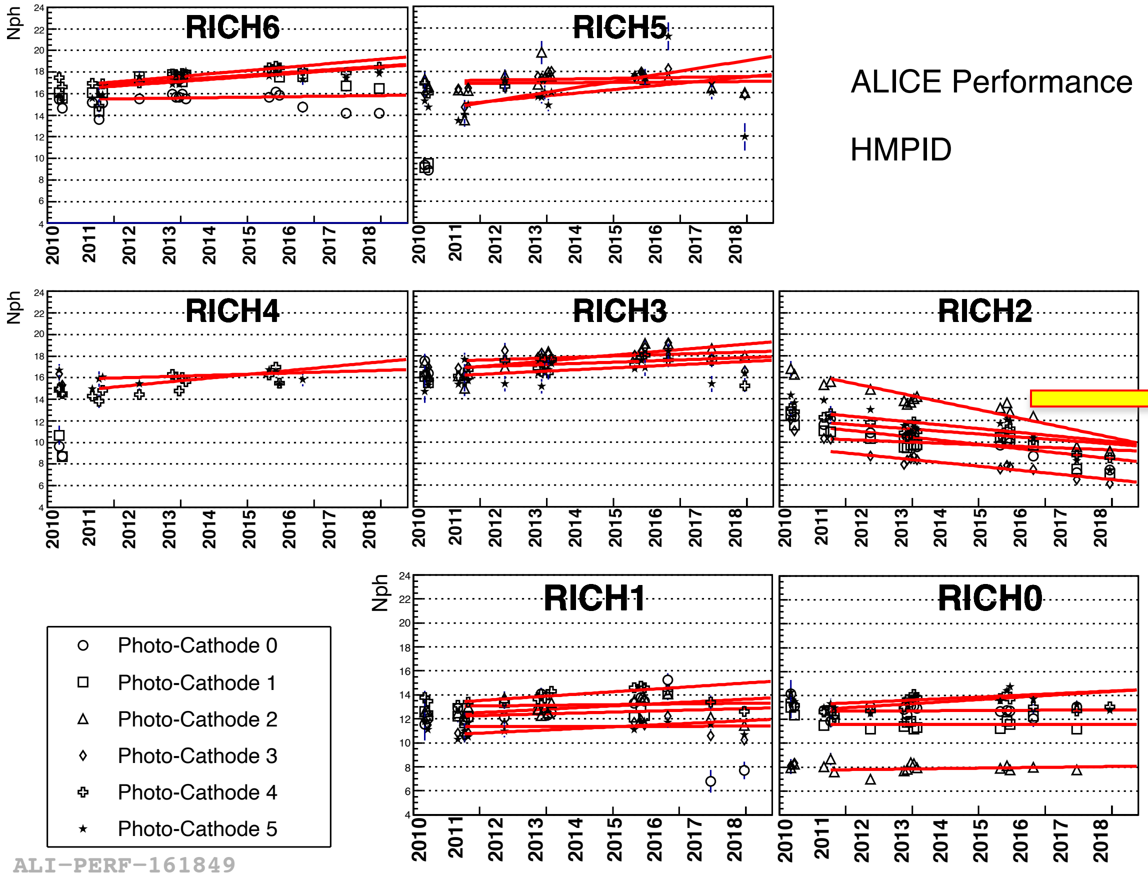

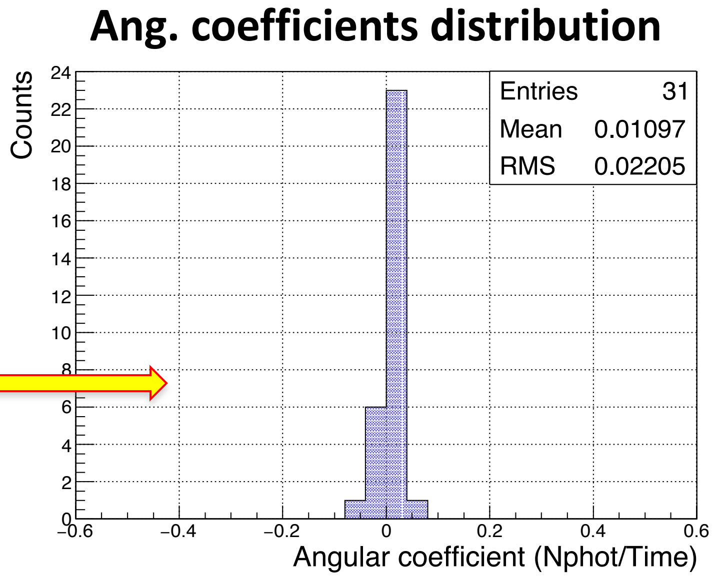

The distribution of the angular coefficients indicates no signs of ageing of the photocathodes!!

- Good N_{ph} stability infers a CsI QE stability;
- Except RICH2, where PC2 and PC3 show a drop of 30%. After cleaning, these PCs were re-evaporated during 2005, maybe procedure not optimised;
- Empty space between blobs represents LHC technical stops from 2010 up to 2015.

Detector stability

Absorbed charge dose for HV sector, period 2010 - 2018

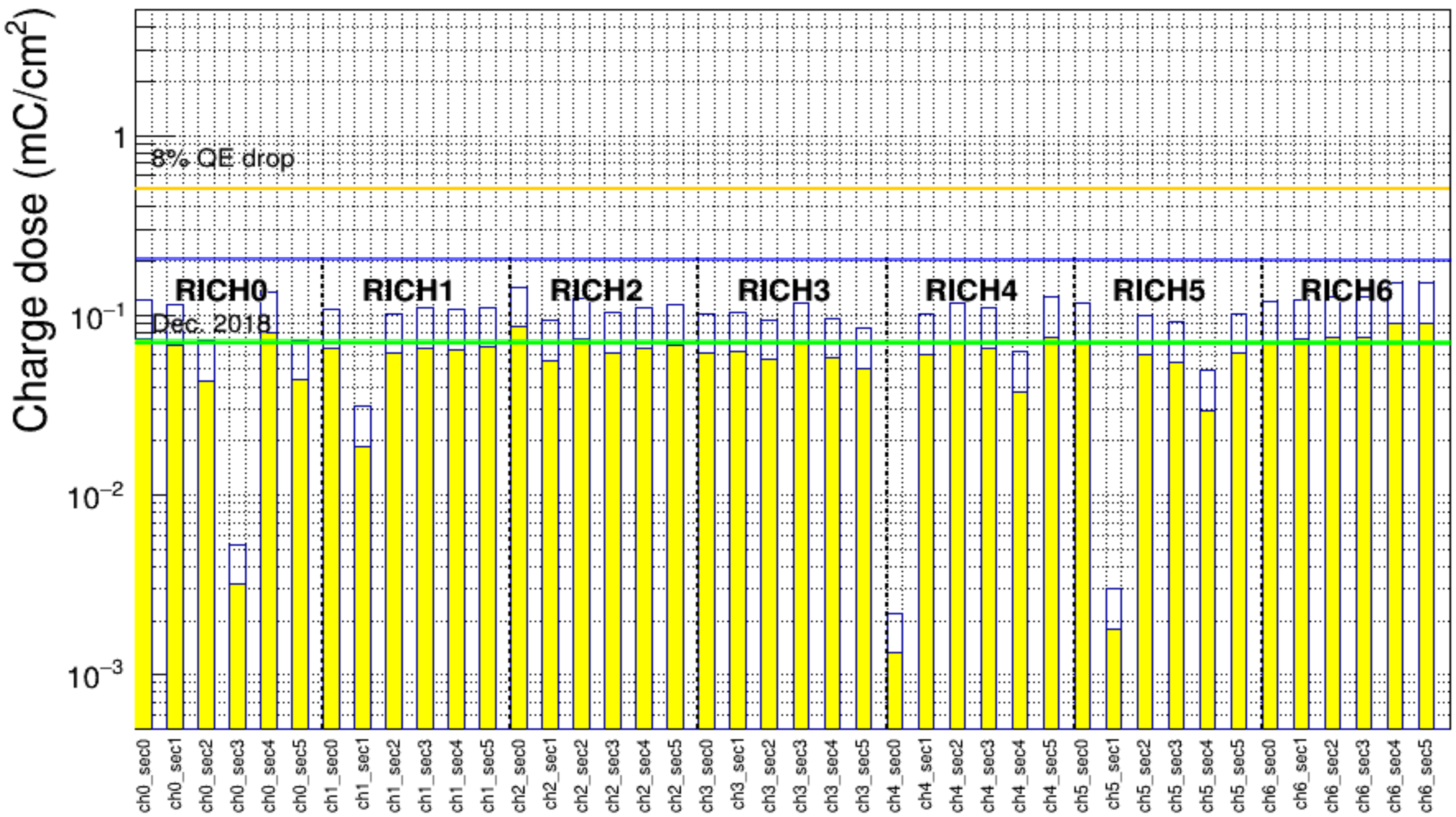

Full yellow bars: measured CsI charge dose end of RUN 2; Empty bars: total anode charge.

Bleu line: dose limit for possible CsI QE loss: 0.2 mC/cm^2; [NIM A553 (2015), NIM A574(2007)]

Orange line: 0.44 mC/cm^2 Expected charge dose end RUN 3. Possible CsI QE loss of 8%.

C_6F_{14} leaks in the radiator vessels

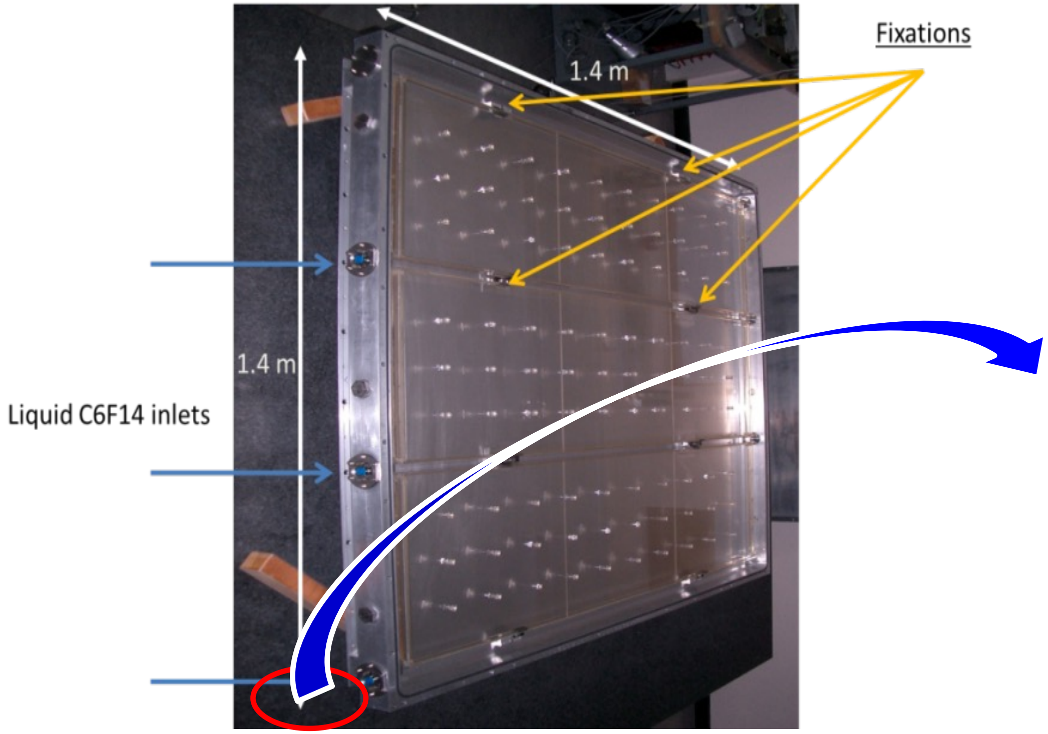

3 radiator vessels 1330x 413 mm² x 15 mm /module

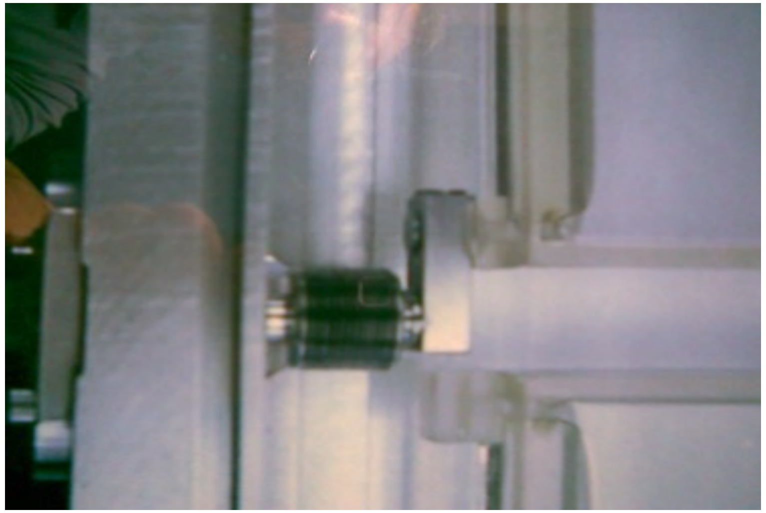

C6F14 inlet fitting (chicane element)

- 21 quartz-NEOCERAM radiator vessels 1330x 413 mm^2 x 15 mm for the 7 modules. All the elements are glued with Araldite 2011;
- Left photo: final assembly and layout in the backplane of one RICH module;
- right photo: stainless steel inlet fitting (chicane element) glued on the NEOCERAM element of the vessels;

Detector status 2022

Leaking radiator vessels

	Year of production YP			
	2002	2003	2004	2005
N° radiators	1	10	5	5

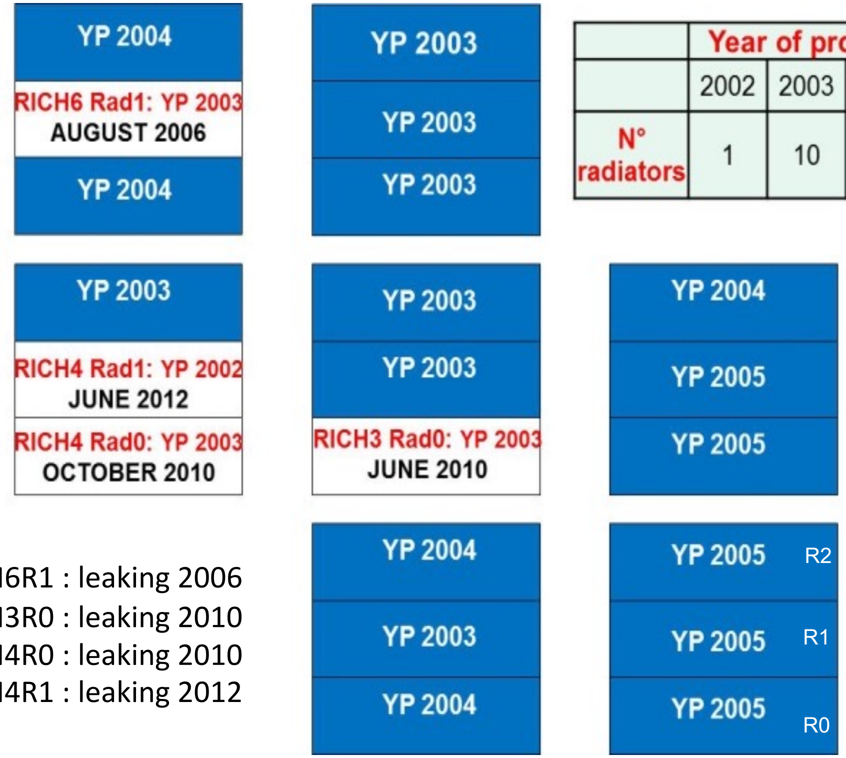

M6R1 : leaking 2006
M3R0 : leaking 2010
M4R0 : leaking 2010
M4R1 : leaking 2012

HV failing sector

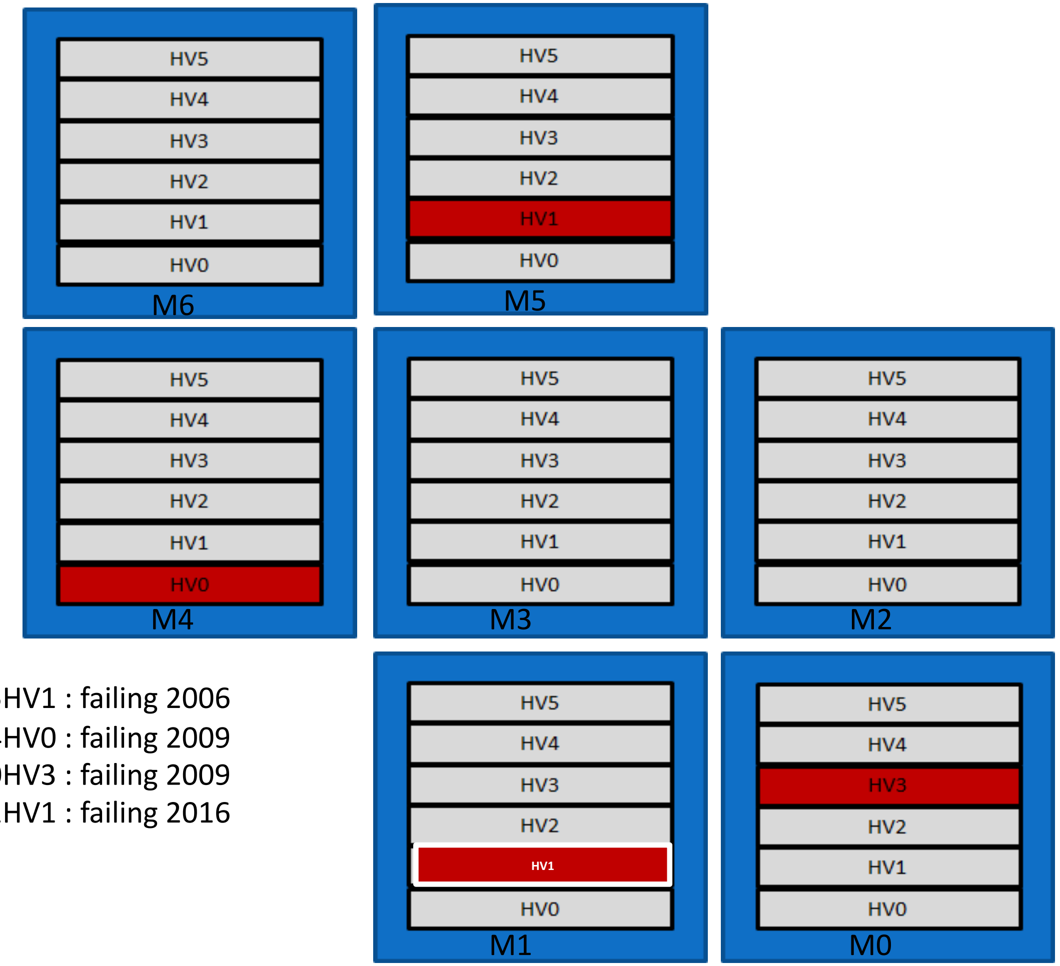

M5HV1 : failing 2006
M4HV0 : failing 2009
M0HV3 : failing 2009
M1HV1 : failing 2016

Faulty sub-system segments:
Combining leaking vessels and failing HV sectors, the detector acceptance is ~ 65%

Readout rate vs. occupancy

- The new RO firmware, the QC and DCS tools are the key components of the excellent performance of the event readout rate;
- These components allow effective and rapid detector configuration and calibration.

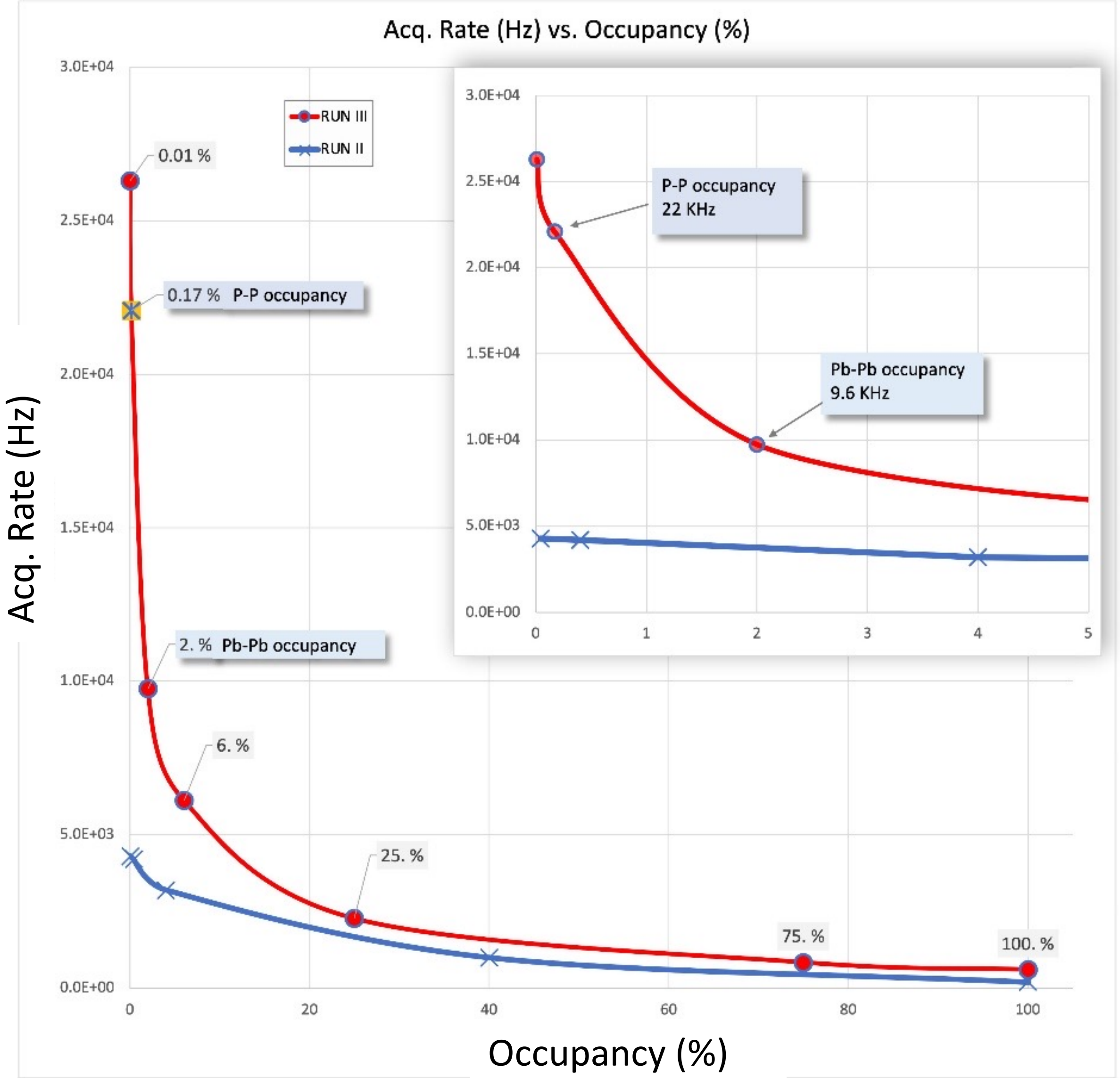

Pattern recognition with HMPID

- A primary track extrapolated from the internal tracking devices has to match with a MIP cluster. This is mandatory for an efficient reconstruction in events with high occupancy in HMPID
- For every cluster in the event, the Cherenkov angle is evaluated (if exists)
- The photon emission angles are reconstructed using a backtracing loop method

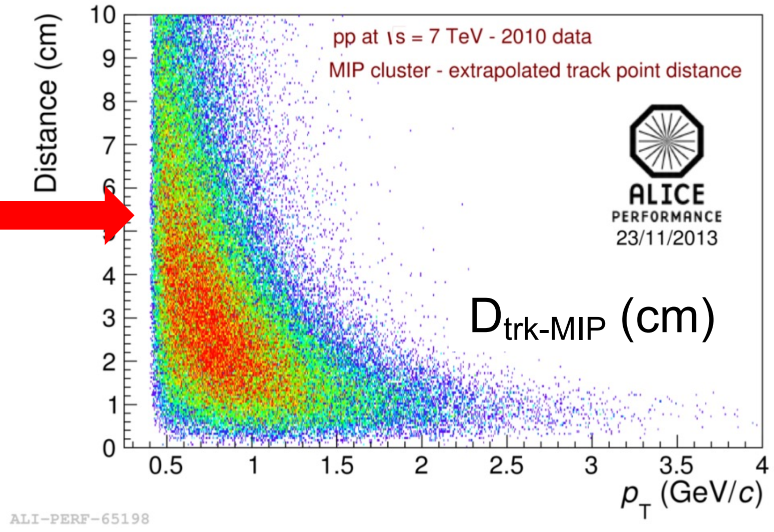

impact track parameter

$$(x,y) \rightarrow ((x_p, y_p, \theta_p, \varphi_p), \eta_c)$$

cluster coordinate

Cherenkov angle

$\Downarrow$

solution in one dimensional mapping space η_c

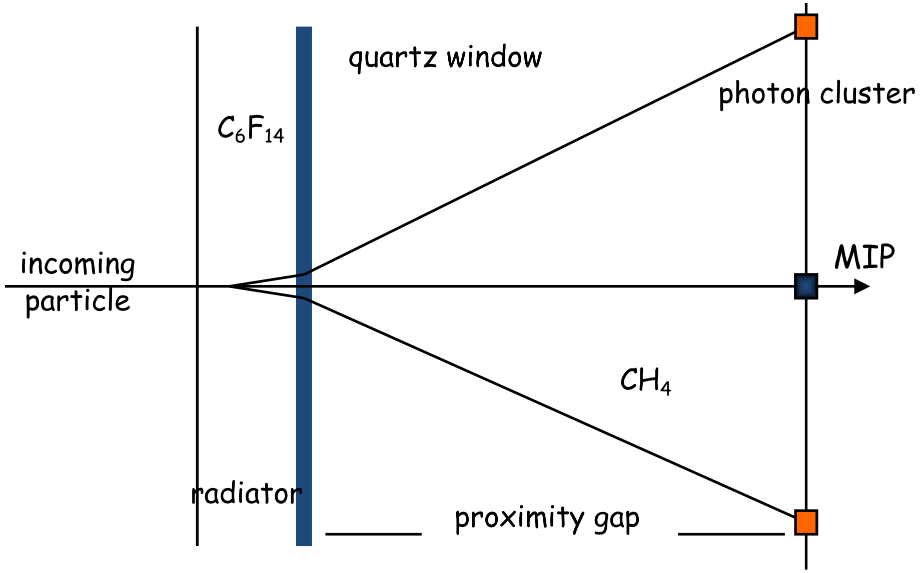

Pattern recognition with HMPID

Background discrimination is performed exploiting the Hough Transform Method (HTM).

• HTM is an efficient implementation of a generalized *template matching* strategy for detecting complex patterns in binary images.

• The starting point of the analysis is a bi-dimensional map with the impact point (x_p, y_p) of the charged particles, hitting the detector plane with known incidence angles (θ_p, φ_p), and the coordinates (x, y) of hits due to both Cherenkov photons and background sources.

• A "Hough counting space" is constructed for each charged particle, according to the following transform: $(x, y) \rightarrow ((x_p, y_p, \theta_p, \varphi_p), \eta_c)$

• (x_p, y_p, θ_p, φ_p) is provided by the tracking of the charged particle, so the transform will reduce the problem to a solution in a one-dimensional mapping space.

• A η_c bin with a certain width is defined. The Cherenkov angle θ_c of the particle is provided by the average of the η_c values that fall in the bin with the largest number of entries

Tracking procedure

The HMPID is located ~5 m from the primary vertex, hence tracks must be propagated through significant material budget after the TPC (~0.36 X_0, ~0.46 X_0 from beam pipe) with respect to other RICH detectors. Precise knowledge of the track parameters is essential!

Reconstructed tracks are propagated up to the HMPID chambers by means of a dedicated algorithm. Below 2 GeV/c most of the track have a distance between the primary track's intersection points at HMPID plane and the corresponding MIP point, above 2 cm. In the tracking procedure, the running track is picked up at the last TPC point and propagated up to the HMPID through the TRD and TOF.

The extrapolation algorithm considers the energy loss and the dependence of the magnetic field value on the distance from the interaction point. It is possible to exploit the precise knowledge (1 mm precision) of the HMPID MIP information in the track fitting.

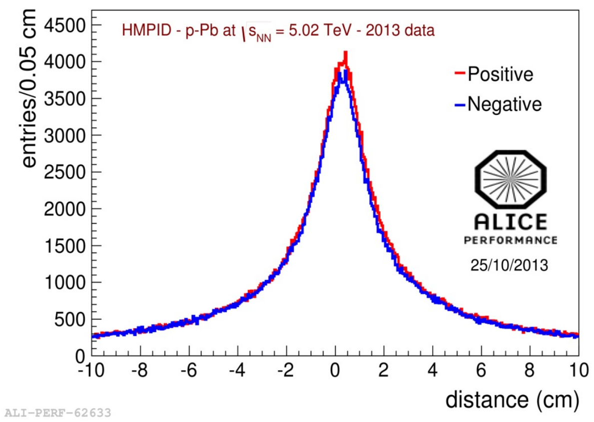

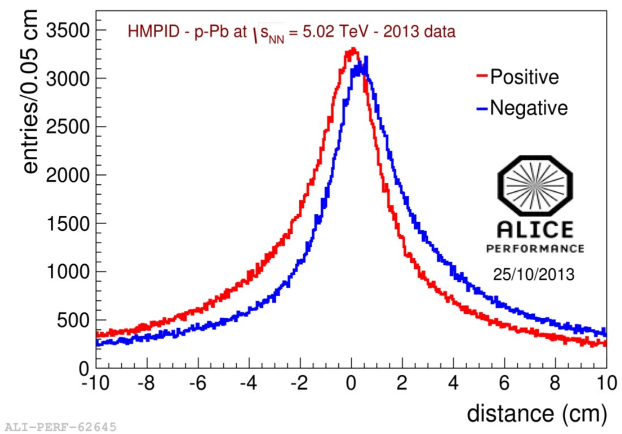

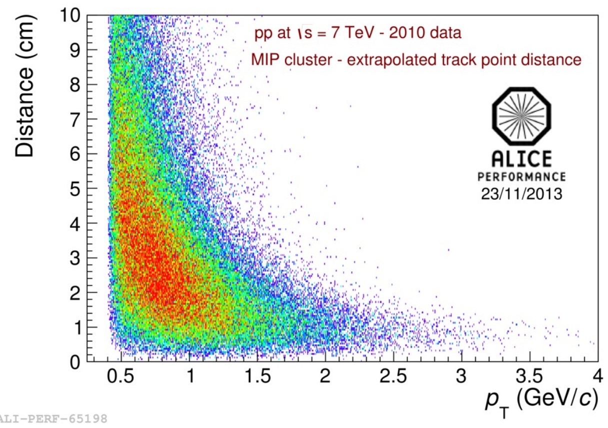

Tracking procedure

Using HMPID MIP clusters information in the tracking procedure improves the track angular resolution, bringing the resolution of the Cherenkov angle close to the design values.

$$sep_{ij}(p_T) = \frac{\langle\theta^i_{Ch}\rangle - \langle\theta^j_{Ch}\rangle}{(\sigma_i + \sigma_j)/2}$$

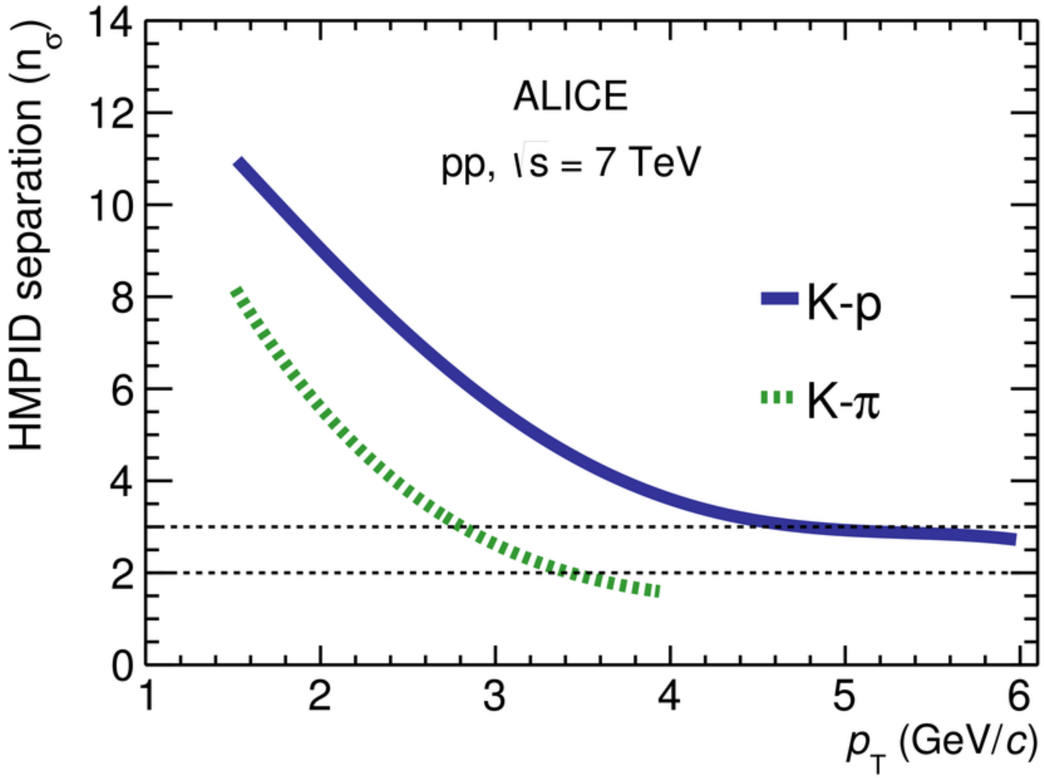

Low multiplicity events, B = 0.5 Tesla

pp at 13 TeV

Gaussian response function

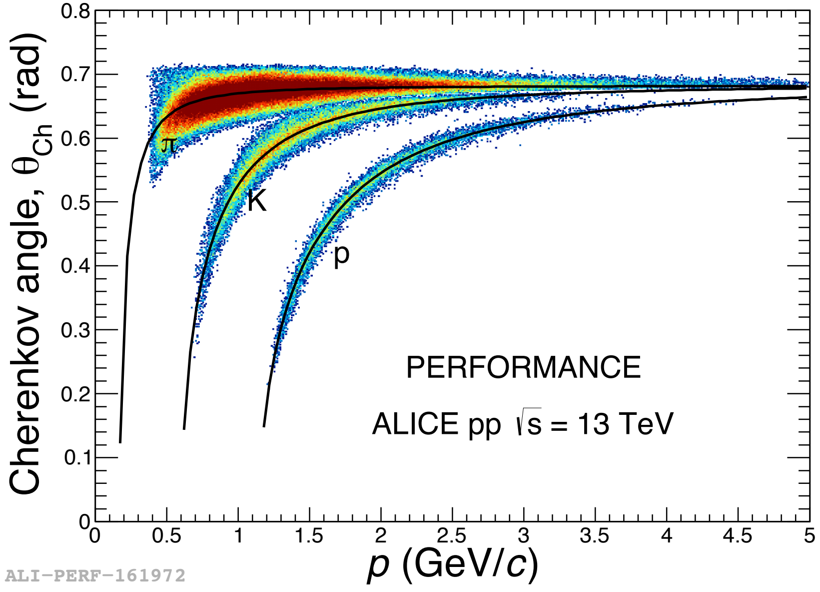

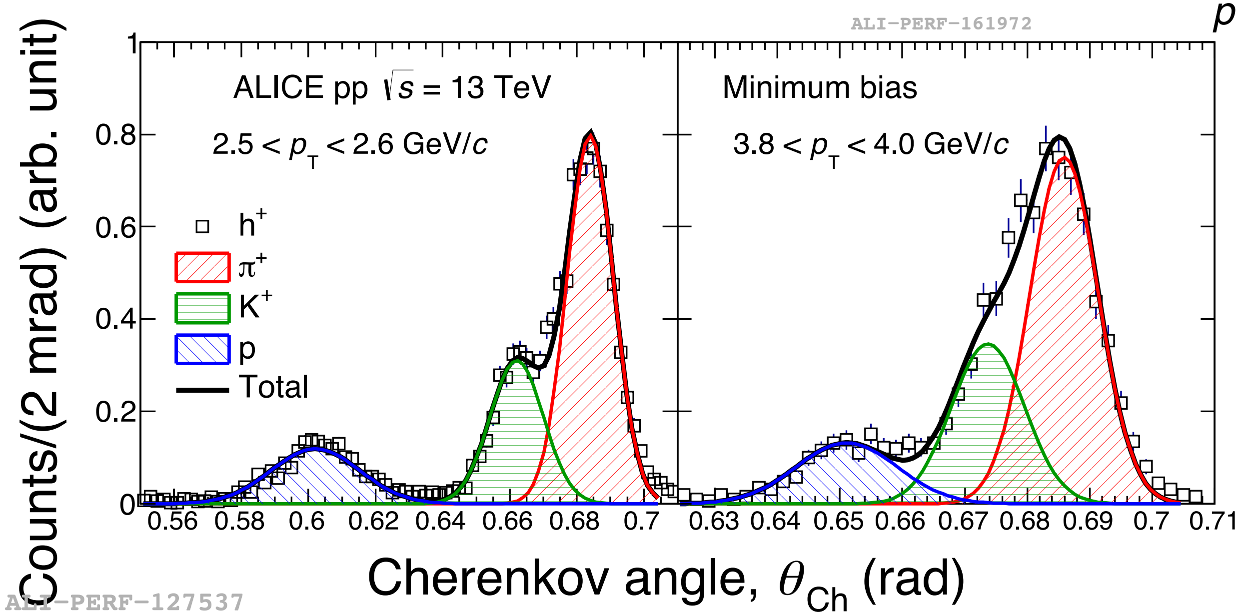

Low multiplicity events, B = 0.2 Tesla

pp at 13 TeV
B = 0.2 Tesla

Gaussian response function

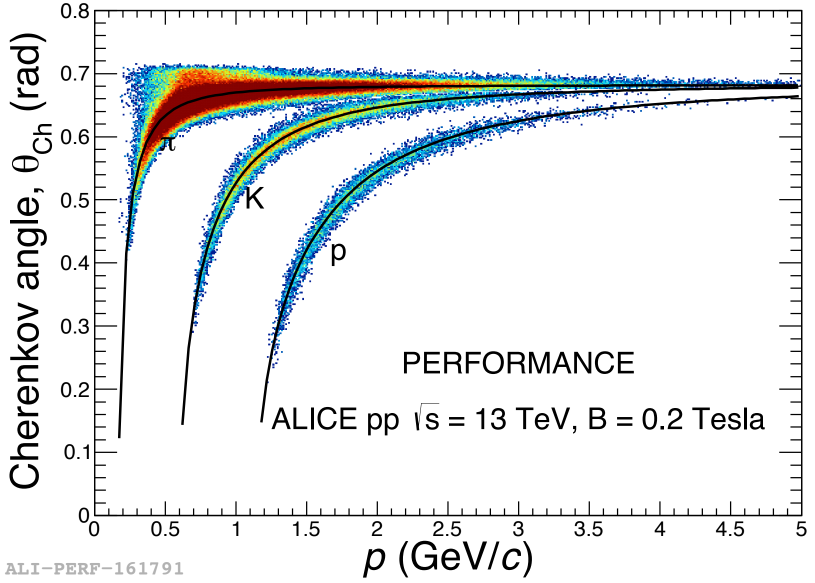

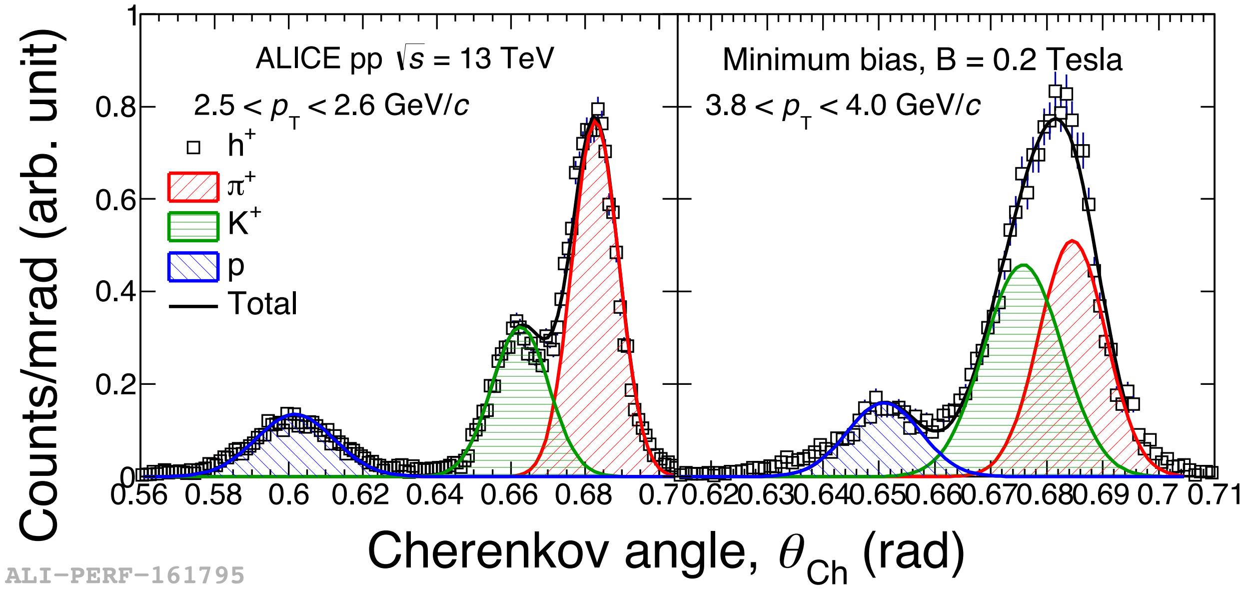

Low multiplicity events: B = 0.2 and 0.5 Tesla comparison

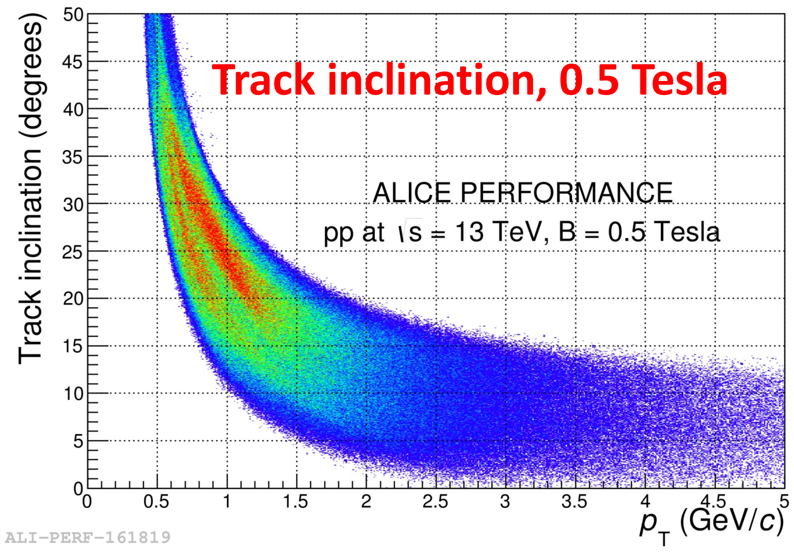

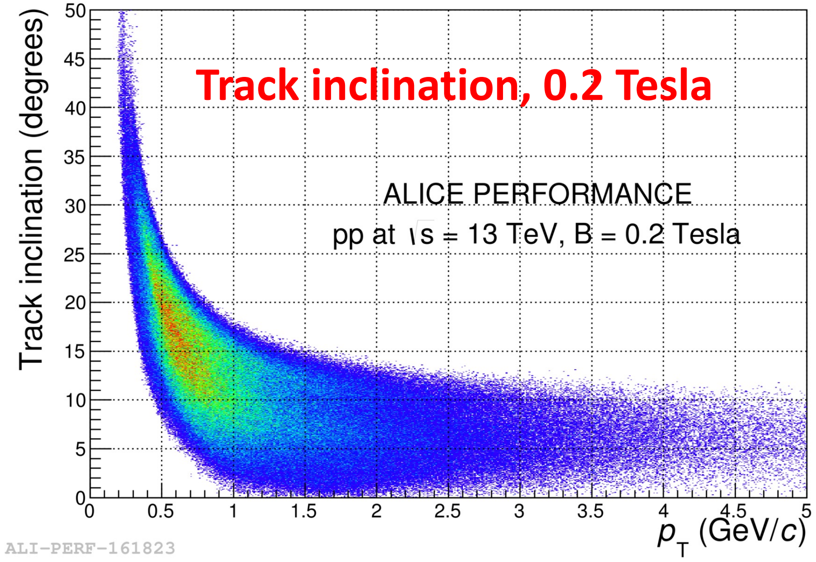

$\sigma_{\theta,\,0.5\,\mathrm{T}} \approx 10$ mrad

$\sigma_{\theta,\,0.2\,\mathrm{T}} \approx 7$ mrad

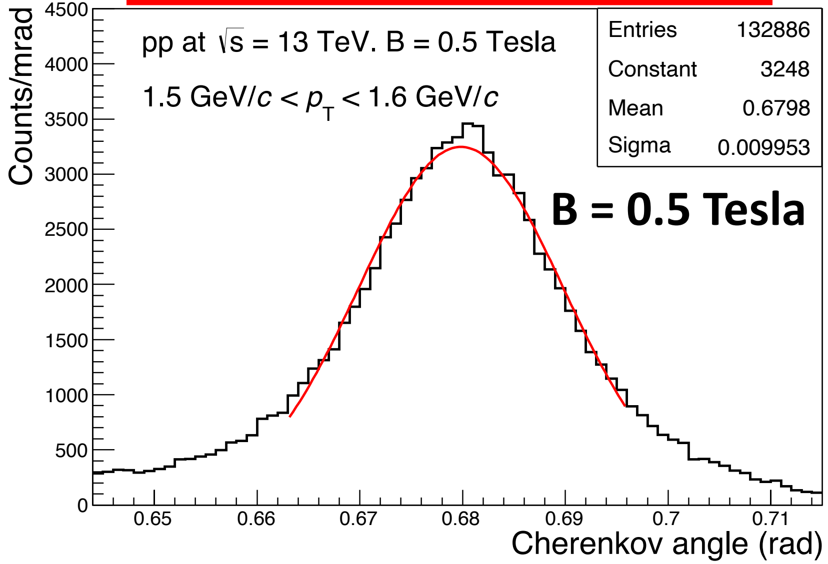

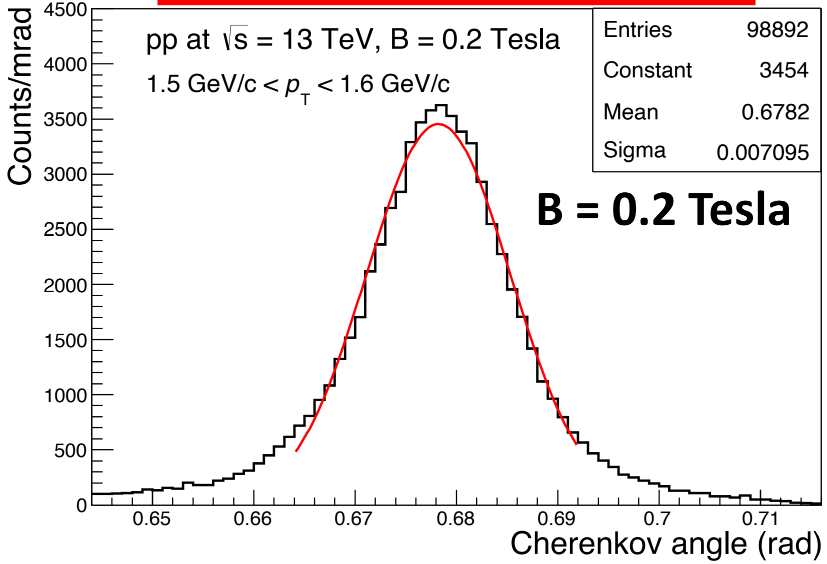

High multiplicity events, B = 0.5 Tesla

Pb-Pb at 5.02 ATeV

Mis–identified tracks (background)

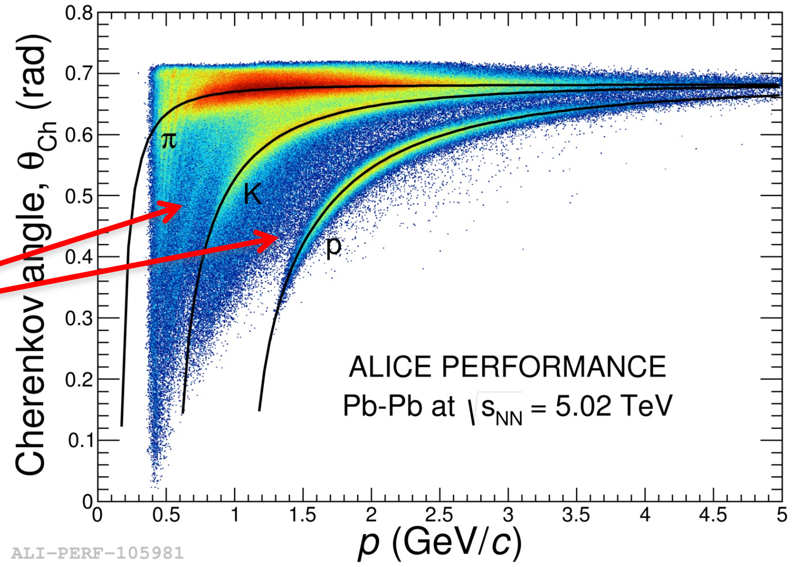

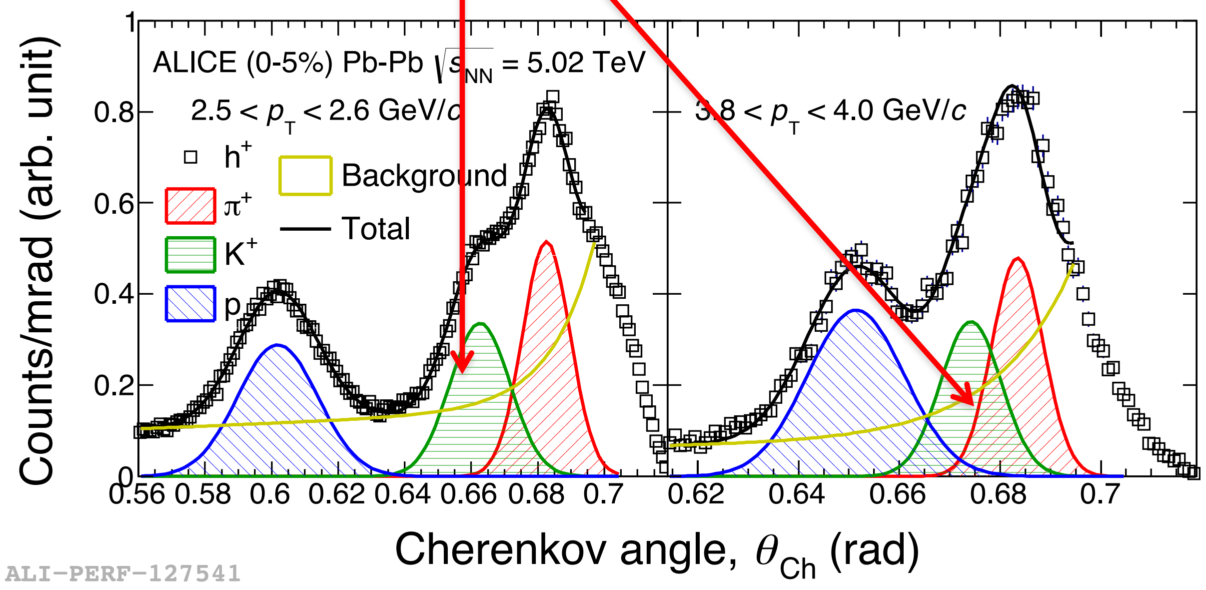

background distribution increases with the Cherenkov angle value;

It is due to mis-identification in the high occupancy events:

- larger is the angle value larger is the probability to find background.

High multiplicity events, B = 0.2 Tesla

Xe-Xe at 5.02 ATeV

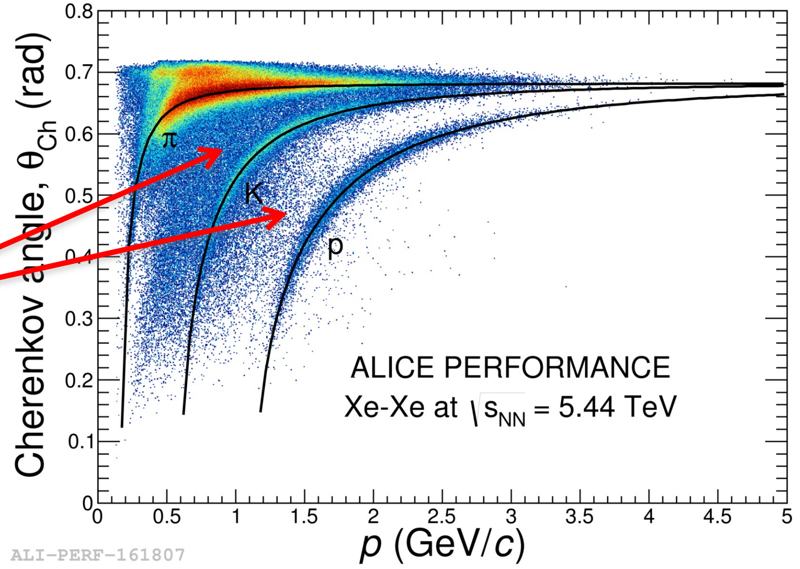

Mis–identified tracks (background)

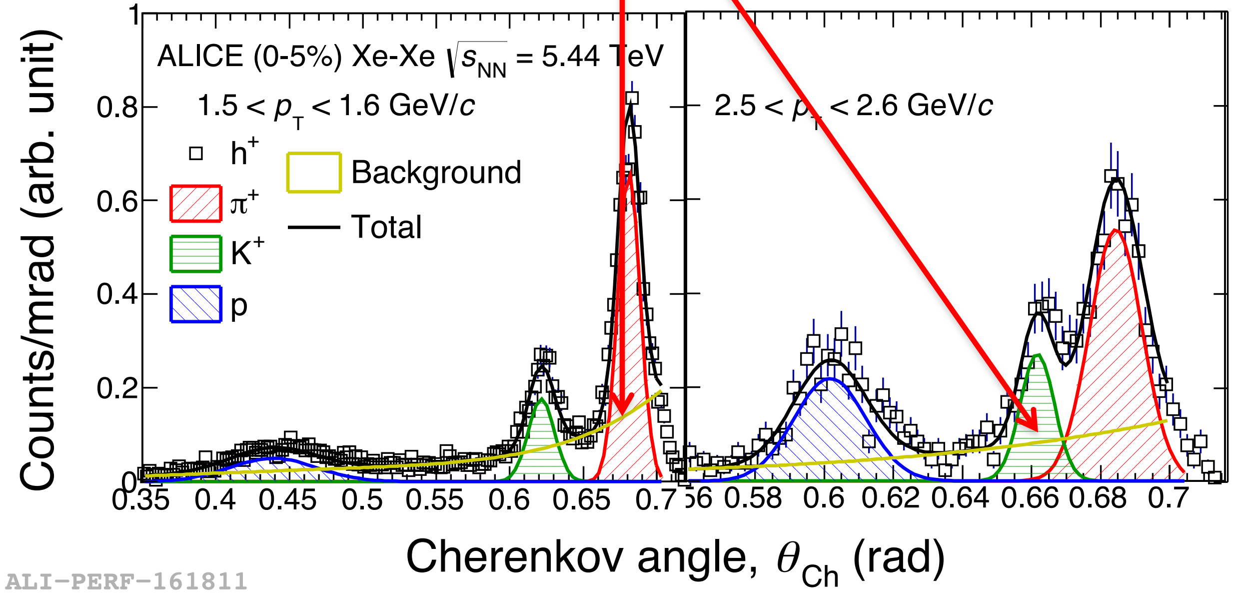

High multiplicity events: B = 0.2 and 0.5 Tesla comparison

Primary track multiplicity in the HMPID acceptance

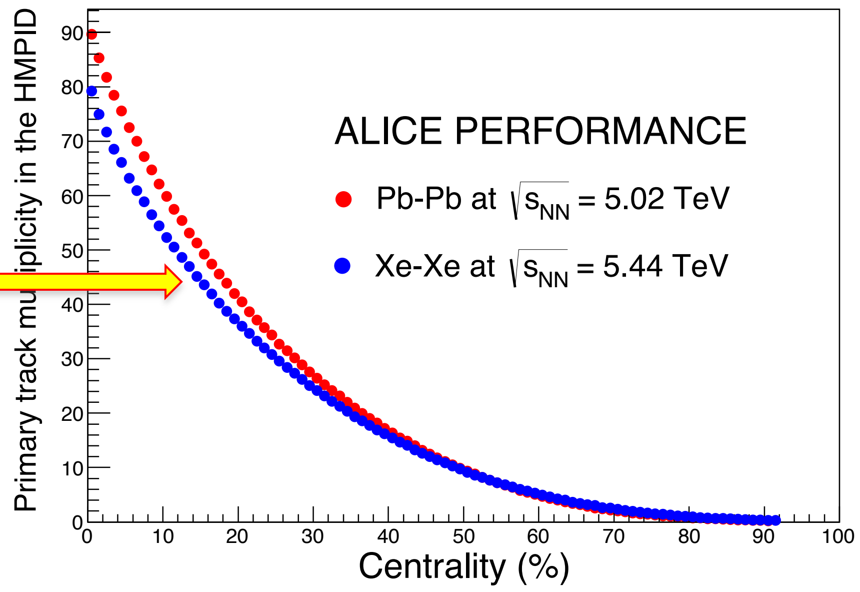

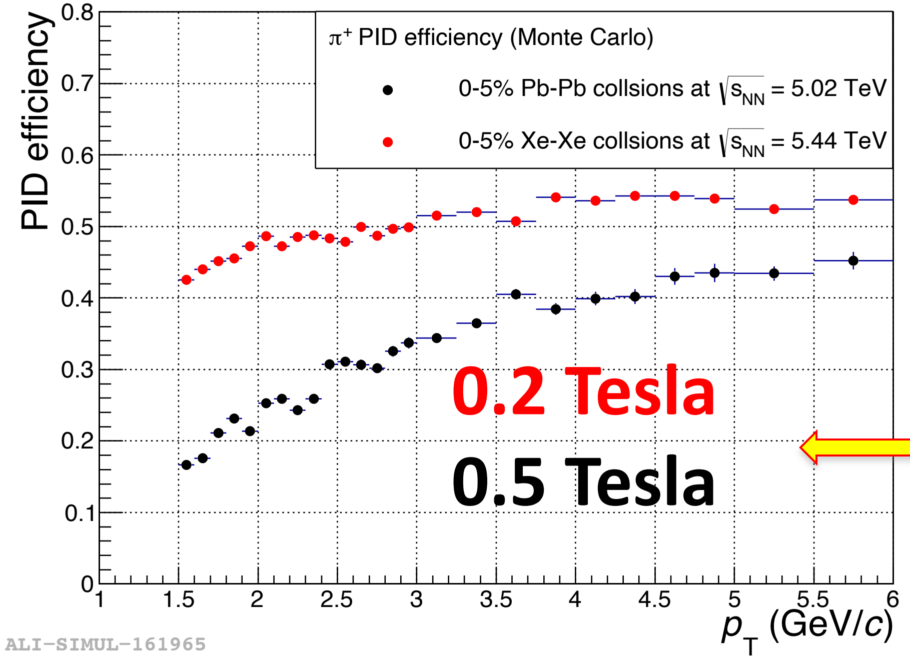

PID *efficiency*

$$\varepsilon_{\mathrm{PID}} = \frac{N(\text{signal})}{N(\text{signal and background})}$$

PID procedure with HMPID

Identification on statistical basis: low multiplicity events

the particle yields are evaluated from a three-Gaussian fit to the Cherenkov angle distribution in a narrow transverse momentum range. The function used is the following:

$$f(\theta) = \frac{Y_\pi}{\sigma_\pi\sqrt{2\pi}} e^{-\frac{(\theta-\langle\theta_\pi\rangle)^2}{2\sigma_\pi^2}} + \frac{Y_K}{\sigma_K\sqrt{2\pi}} e^{-\frac{(\theta-\langle\theta_K\rangle)^2}{2\sigma_K^2}} + \frac{Y_p}{\sigma_p\sqrt{2\pi}} e^{-\frac{(\theta-\langle\theta_p\rangle)^2}{2\sigma_p^2}}$$

$\langle\theta_i\rangle$ = means of the Cherenkov angle distributions
σ_i, = standard deviation of the Cherenkov angle distributions.
Y_i = integral of the single Gaussian functions

- 9 parameters to be calculated, the three mean values, the three sigma values and the three yields.
- Mean and sigma values are know and fixed in the fitting.

pp event display

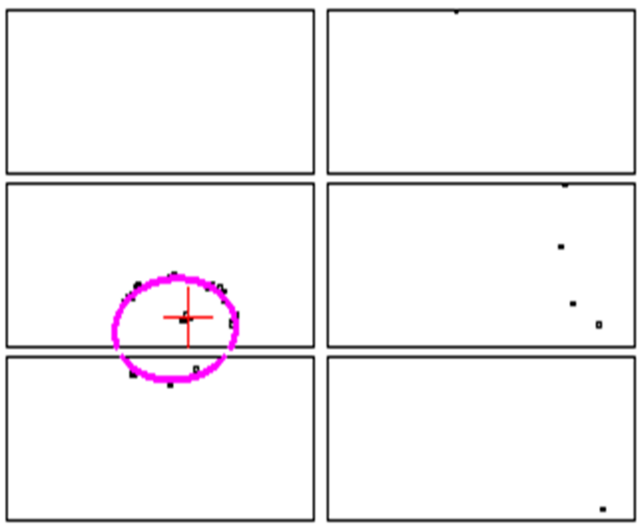

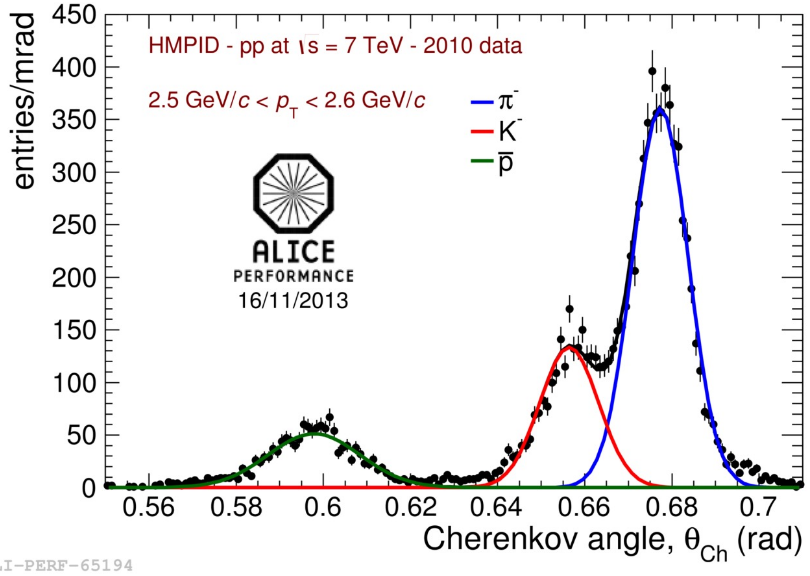

PID procedure with HMPID

Identification on statistical basis: high multiplicity events (central Pb-Pb collisions)

- the three Gaussian distributions in a given transverse momentum bins are convoluted with a background distribution;
- Such distribution increases with the Cherenkov angle value;
- It is due to mis-identification in the high occupancy events:
  - larger is the angle value larger is the probability to find background;
- In the yield extraction procedure, the background function has to be convoluted with the three-Gaussian one.

Pb-Pb event display

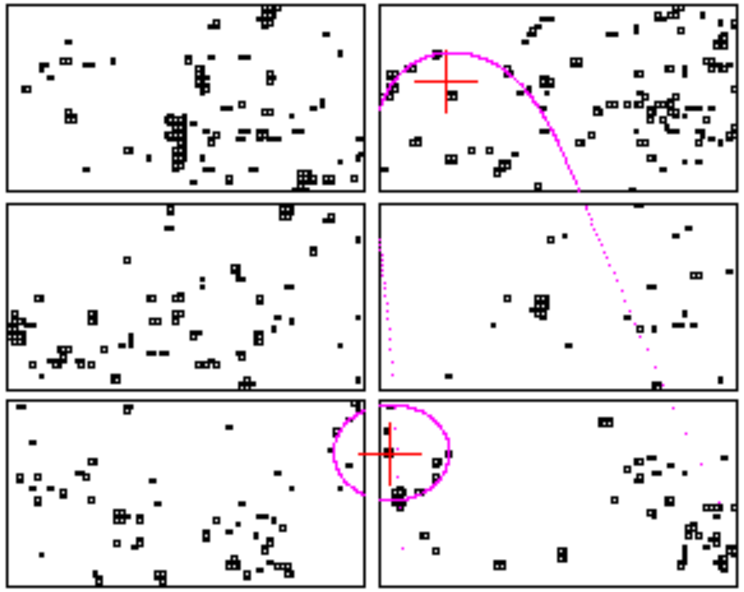

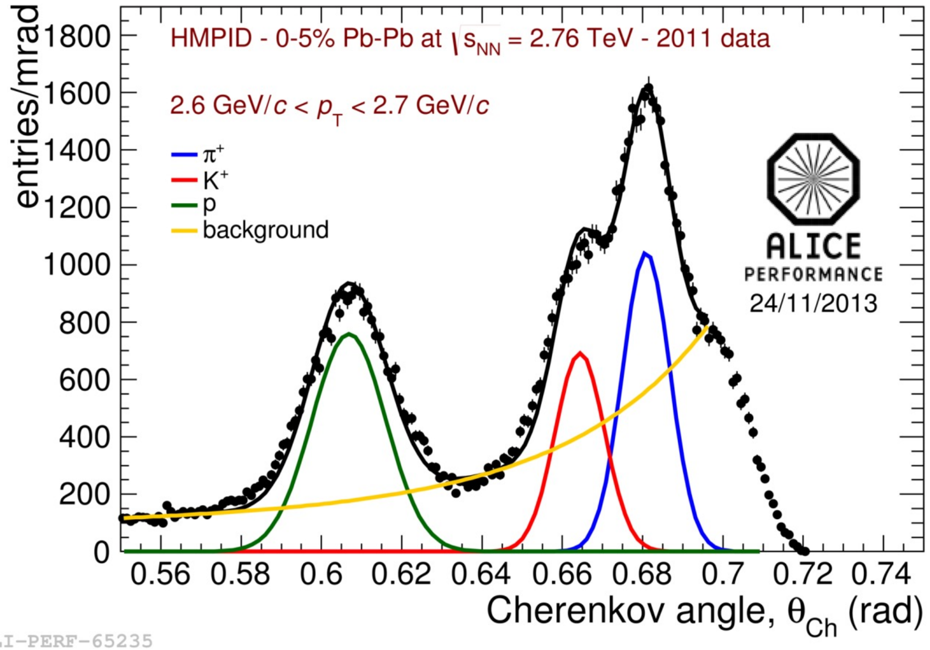

ALI-PERF-65235

PID procedure with HMPID

Identification on track-by-track basis

- From the knowledge of the expected Cherenkov angle value and the expected theoretical standard deviation, it is possible to calculate the values of two PID estimators:
  - the probability to be one of the charged hadron specie;
  - the difference between the measured angle value and the expected theoretical one in sigma units;

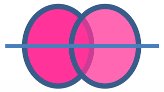

$$N_{sigmas} < 2$$

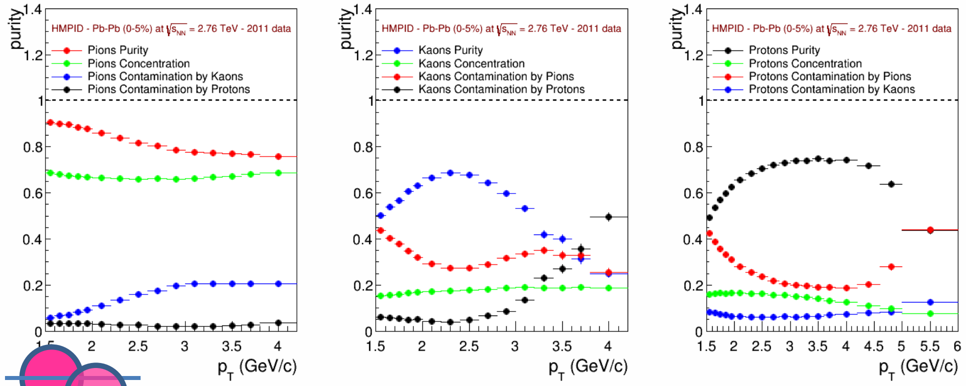

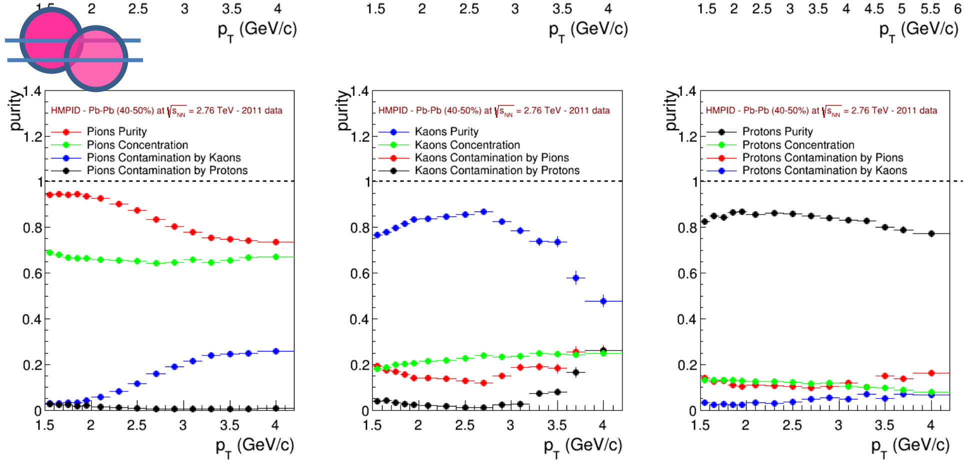

$$N^i_{sigmas} = \frac{\left|\theta_{\exp} - \theta^i_{theor}\right|}{\sigma^i}$$

$$p_i = \frac{N^t_{id}(i)}{N_{id}(i)} \qquad c_i = \frac{N^w_{id}(i)}{N_{id}(i)}$$

$$i = \pi, K, p$$

p_i = purity, c_i = contamination
$N_{id}(i)$ = number of particles identified as type i
$N_{id}^t(i)$ = number of true particles of type i identified as type i
$N_{id}^w(i)$ = number of non-type i particles identified as particles of type i

Deuterons identification: Pb-Pb 5.02 ATeV

$$m^2 = p^2(n^2\cos^2\theta_{ckov} - 1)$$

n = refractive index

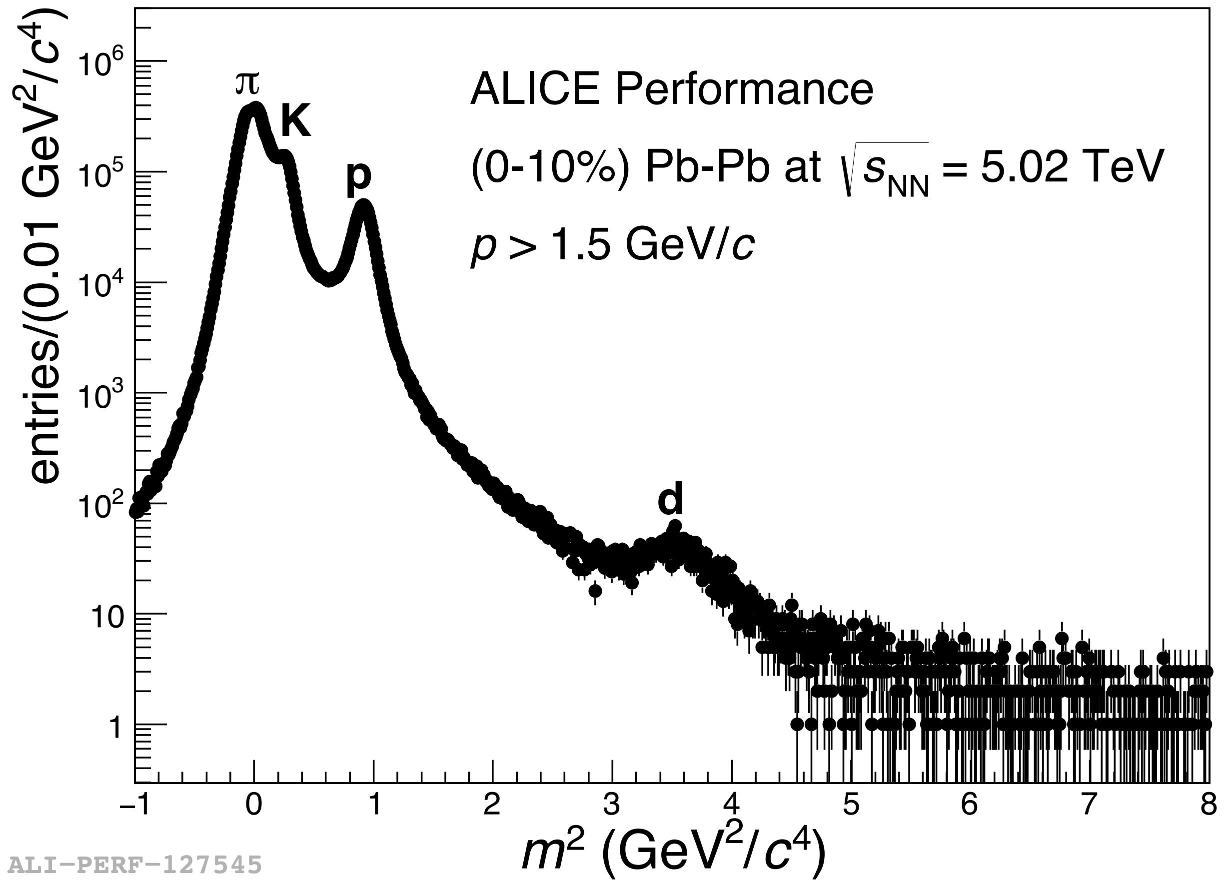

Conclusion

- The HMPID detector is installed in the ALICE cavern since September 2006.

- The detector has exhibited satisfactory performance, meeting the requirements outlined for the planned physics programs in both Run 1 and Run 2.

- In Run 3 the HMPID readout rate is 20 KHz in pp collisions and 9 KHz in Pb-Pb, 10 times higher the rate limited by the triggered TPC in Run 1 and 2.

- The Detector is compliant with the new Online and Offline ALICE data taking and analysis environment (O^2). Now the TPC is on continuous RO!!

Issues experienced so far

- The PID efficiency in a high multiplicity environment has fallen below the expected levels, primarily due to deviations in the magnetic field strength. Initially set at 0.2 T, the magnetic field increased to 0.5 T, negatively impacting the pattern recognition performance of HMPID.

- A significant vulnerability emerged in the form of the liquid radiator vessels, leading to structural weaknesses and subsequent vessel failures. Regrettably, during the detector design phase, the chemical interaction between C6F14 and araldite was not considered, contributing to the challenges encountered.

Backup

ALICE charged hadrons yields evaluation strategy

- To measure the production of pions, kaons and protons over a wide p_T range, results from five different independent PID techniques/detectors, namely ITS, TPC, TOF, HMPID and kink-topology (for kaons), are combined.

- In their overlap p_T regions the spectra from the different PID techniques are consistent within uncertainties:
    - the results are combined in the overlapping ranges using a weighted mean with the independent systematic uncertainties as weights.

- The HMPID constrains the uncertainty of the measurements in the transition region between the TOF and TPC relativistic rise methods (around p_T = 3 GeV/c). It both improves the precision of the measurement and validates the other methods in the region where they have the worst PID separation.

HMPID separation power in σ unit as a function of p_T

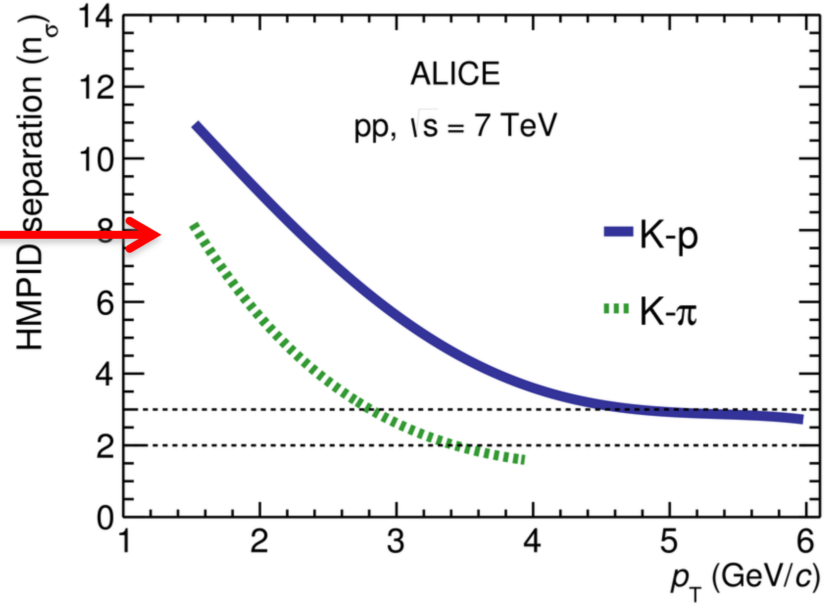

Charged hadrons spectra: pp 7 TeV

Eur. Phys. J. C (2015) 75:226

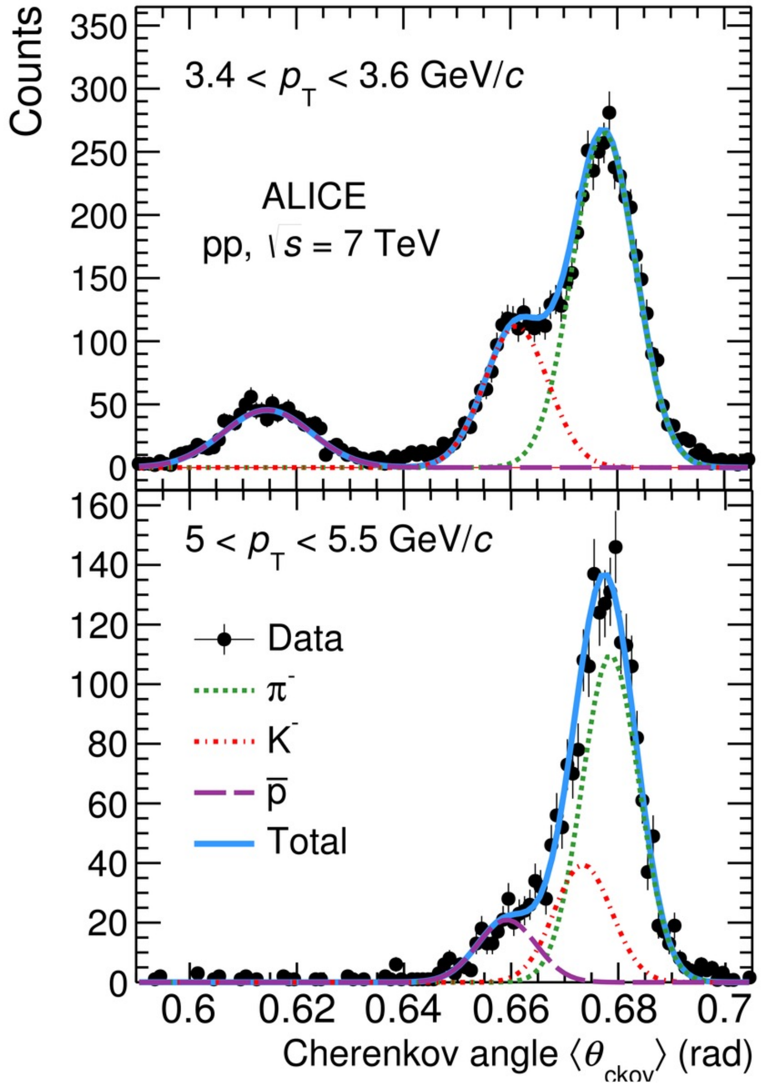

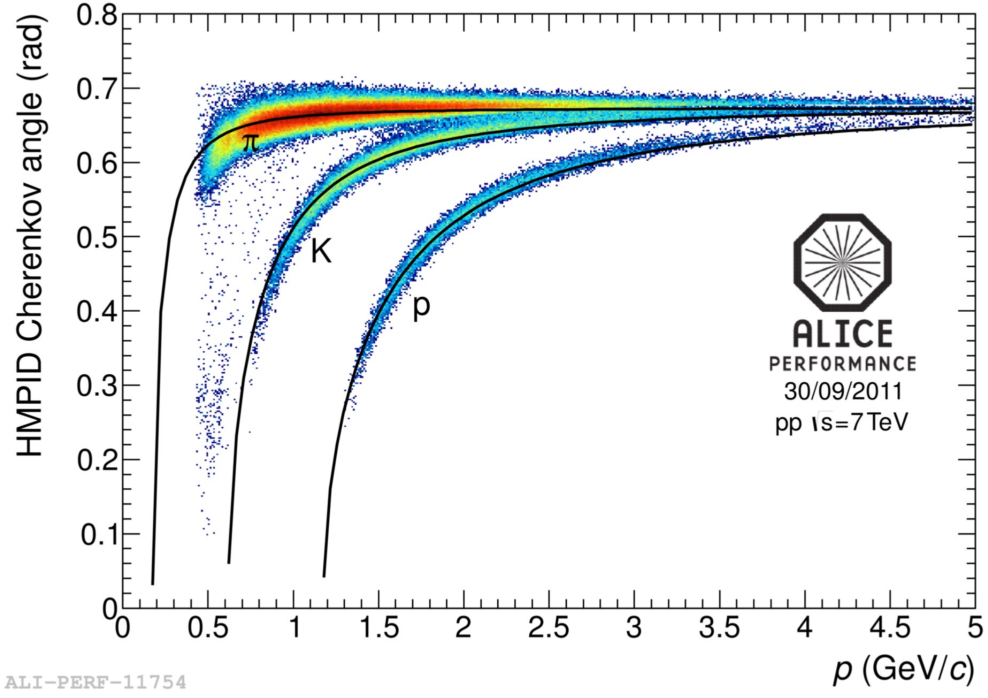

PID range

$\pi/K \rightarrow 1.5 - 3$ GeV/c

$P \rightarrow 1.5 - 6$ GeV/c

Charged hadrons spectra: pp 7 TeV

π/K HMPID | p HMPID

π, K and p spectra, resulting from the combination of the information provided by 5 different analyses (dE/dx, TOF, Cherenkov, kinks topology for kaons).

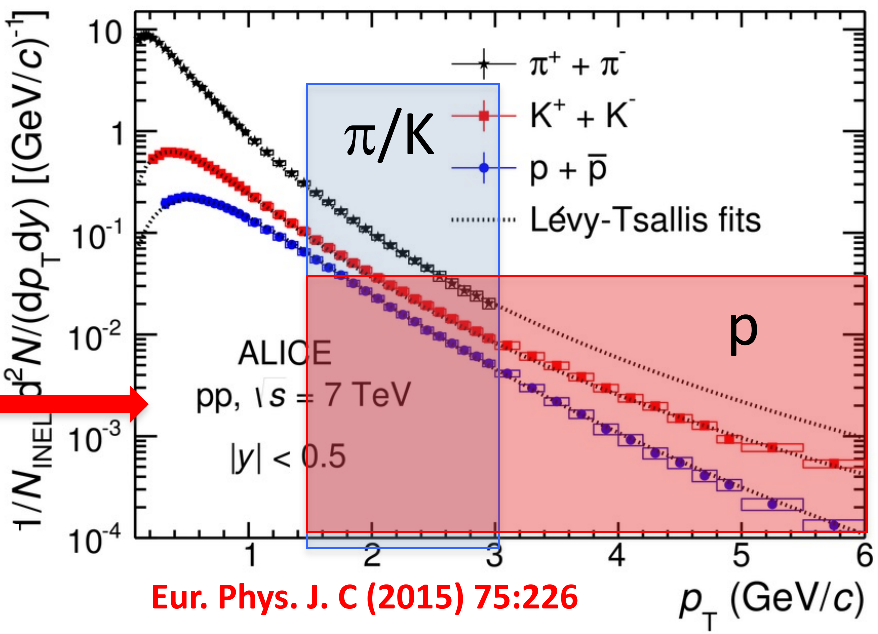

Eur. Phys. J. C (2015) 75:226

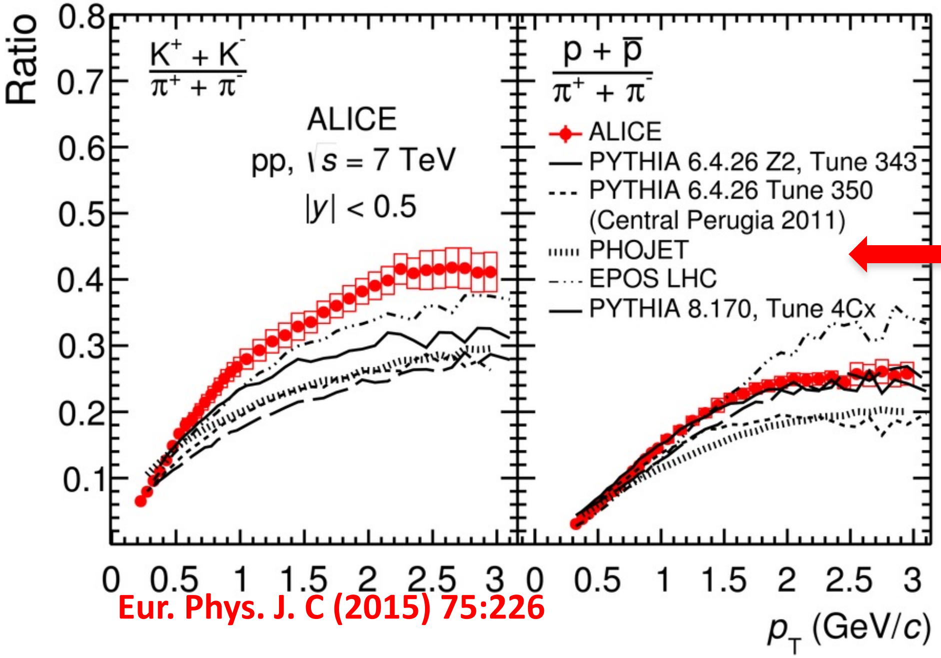

Eur. Phys. J. C (2015) 75:226

- $(K^+ + K^-)/(\pi^+ + \pi^-)$ and $(p + p)/(\pi^+ + \pi^-)$ ratios as a function of p_T compared with some event generators.
- $(K^+ + K^-)/(\pi^+ + \pi^-)$ ratio increases from 0.05 at p_T = 0.2 GeV/c up to 0.45 at $p_T \sim$ 3 GeV/c with a slope that decreases with increasing p_T.

Charged hadrons spectra: Pb-Pb 2.76 ATeV

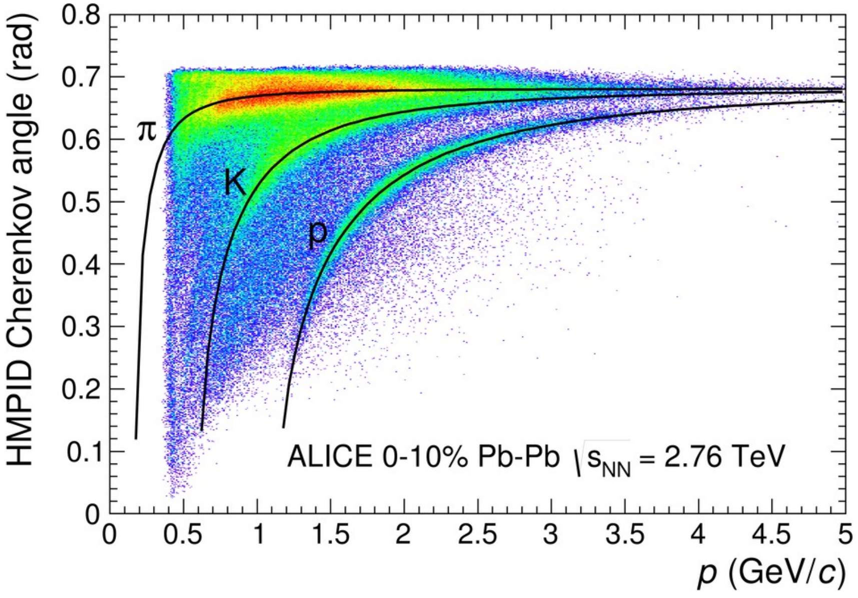

Performance

PID range

π/K → 1.5 – 4 GeV/c

p→1.5 – 6 GeV/c

PHYSICAL REVIEW C 93, 034913 (2016)

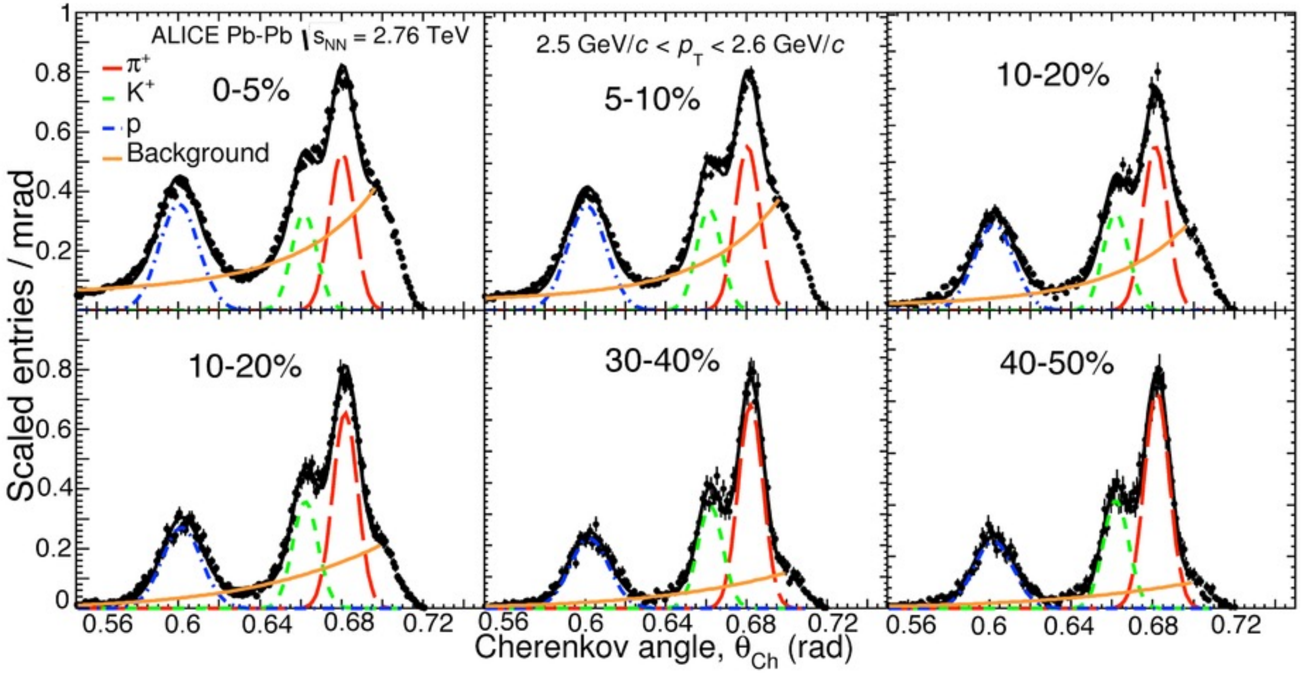

- HMPID used in collisions centrality range 0-50%
- Centrality estimate based on V0 detector measurements.
- V0: trigger detector at forward rapidity.

Charged hadrons spectra: Pb-Pb 2.76 ATeV

Performance

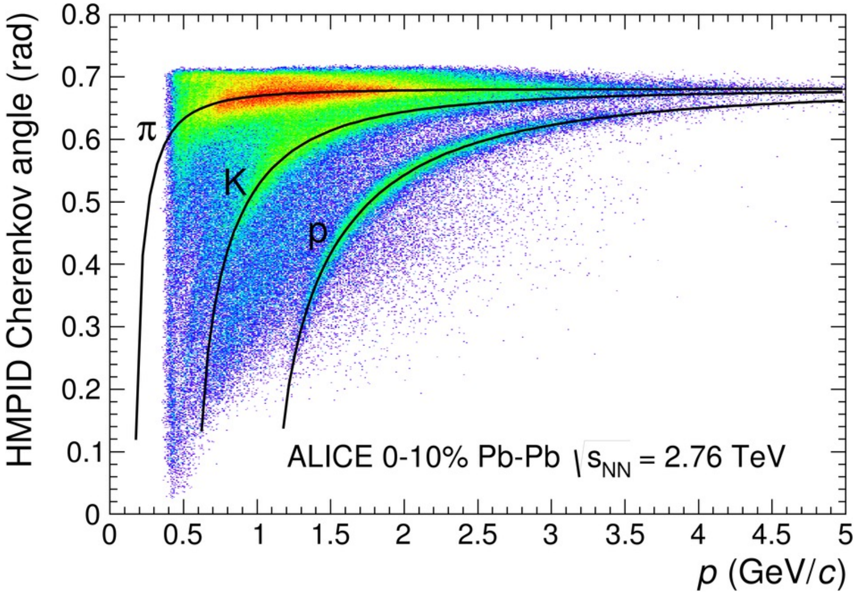

PID range

π/K → 1.5 – 4 GeV/c

p→1.5 – 6 GeV/c

PHYSICAL REVIEW C 93, 034913 (2016)

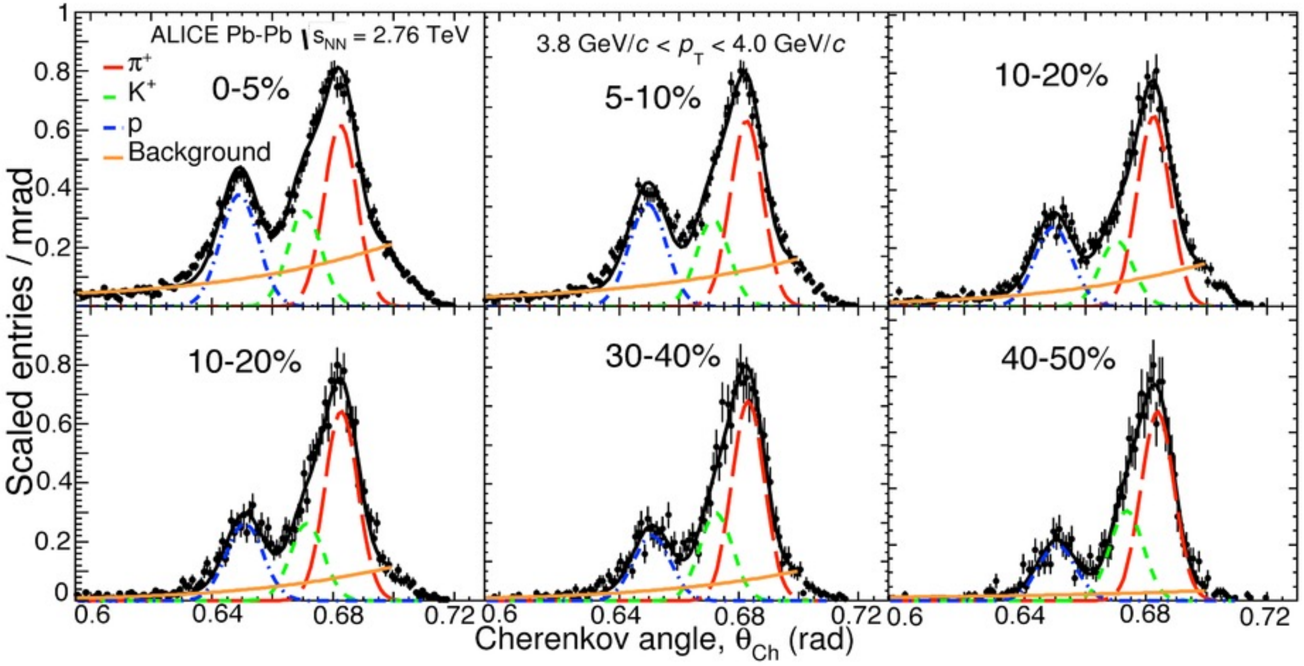

- HMPID used in collisions centrality range 0-50%
- Centrality estimate based on V0 detector measurements.
- V0: trigger detector at forward rapidity.

Charged hadrons spectra: Pb-Pb 2.76 ATeV

- For p_T < 3 GeV/c a hardening of the spectra is observed going from peripheral to central events. This effect is mass dependent and is characteristic of hydrodynamic flow.

- For high p_T (>10 GeV/c) the spectra follow a power law shape as expected from pQCD.

PHYSICAL REVIEW C 93, 034913 (2016)

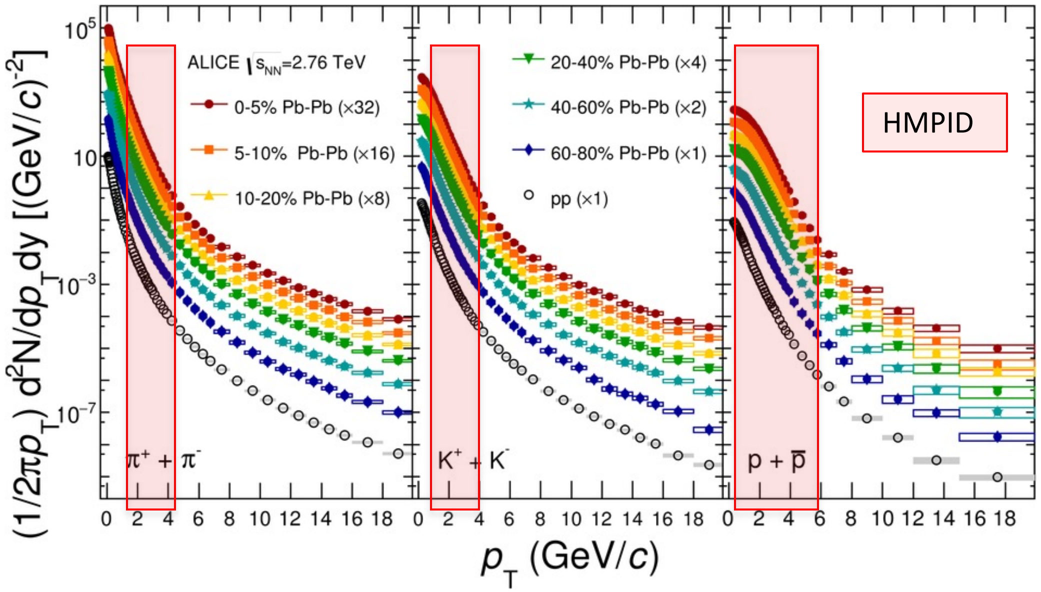

PHYSICAL REVIEW C 93, 034913 (2016)

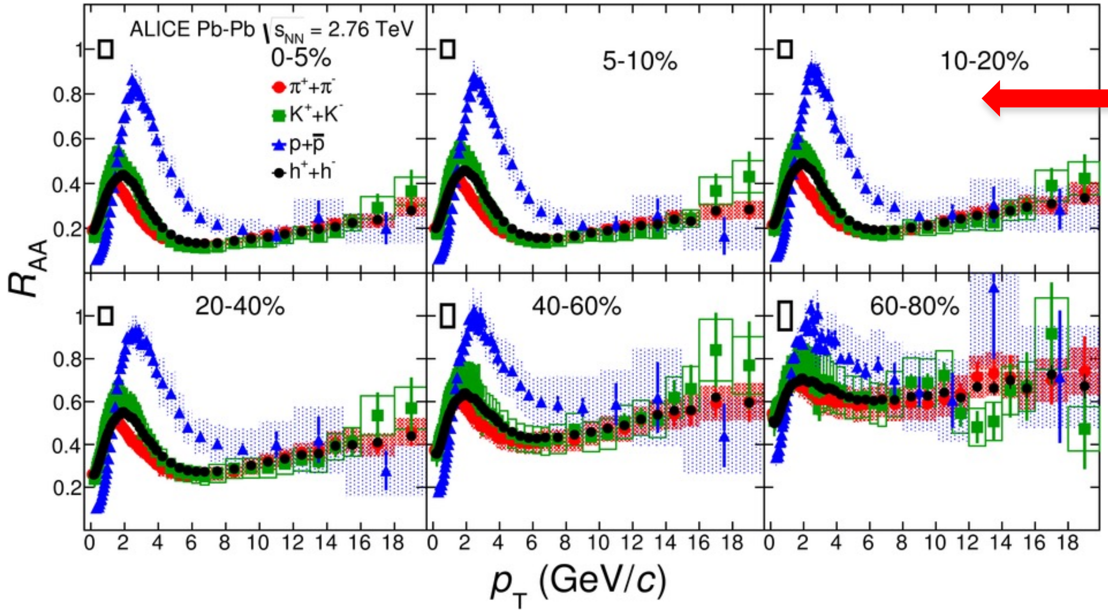

$$R_{AA} = \frac{d^2N_{\mathrm{id}}^{AA}/dy\,dp_T}{\langle T_{AA}\rangle d^2\sigma_{\mathrm{id}}^{\mathrm{pp}}/dy\,dp_T}$$

- For p_T < ≈ 8 – 10 GeV/c: R_{AA} for π and K are compatible and are smaller than R_{AA} for p.

- At high p_T : R_{AA} for π, K and p are compatible.

Charged hadrons spectra: p-Pb 5.02 TeV

Performance

PID range

π, K: 1.5 – 4 GeV/c
p: 1.5 – 6 GeV/c

Physics Letters B 760 (2016) 720–735

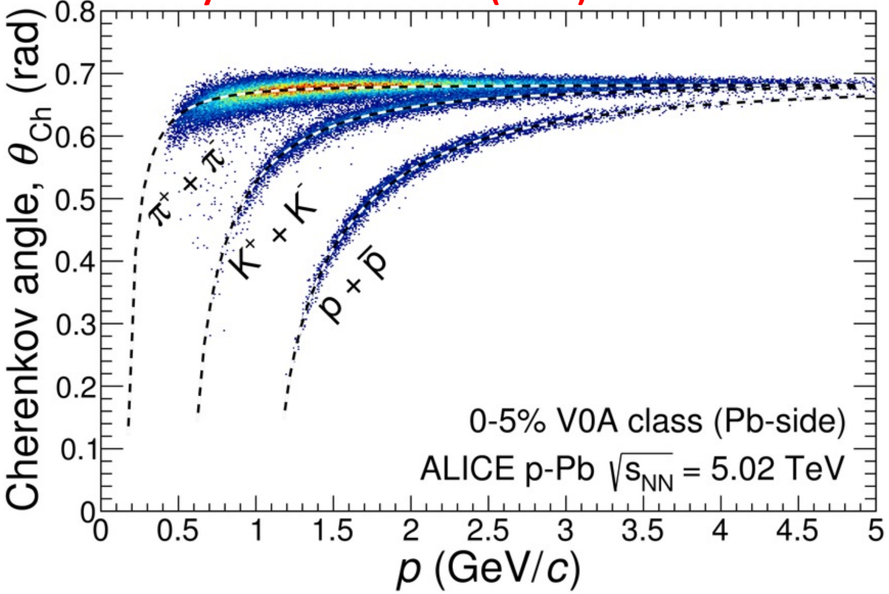

Physics Letters B 760 (2016) 720–735

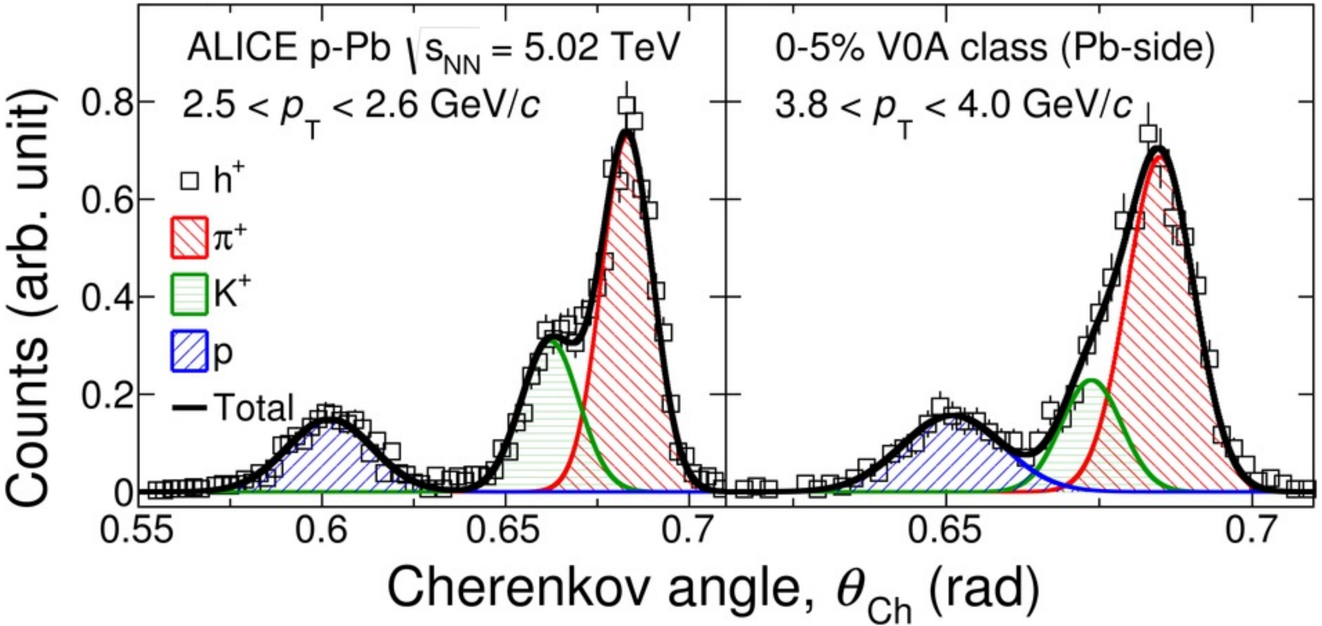

- HMPID used in collisions multiplicity range: 0 – 100 %
- multiplicity estimate based on V0 detector measurements.

Charged hadrons spectra: p-Pb 5.02 TeV

Physics Letters B 760 (2016) 720–735

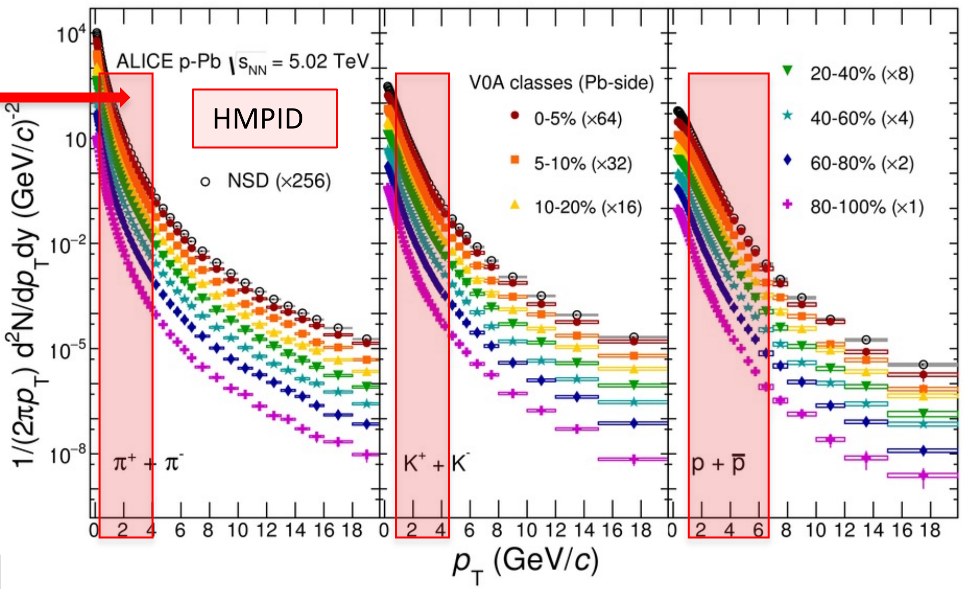

- Hardening with multiplicity and particle mass

- Reminiscent of observed effects in Pb-Pb Attributed to radial flow/recombination (Indication for collective effects in p-Pb?!)

Physics Letters B 760 (2016) 720–735

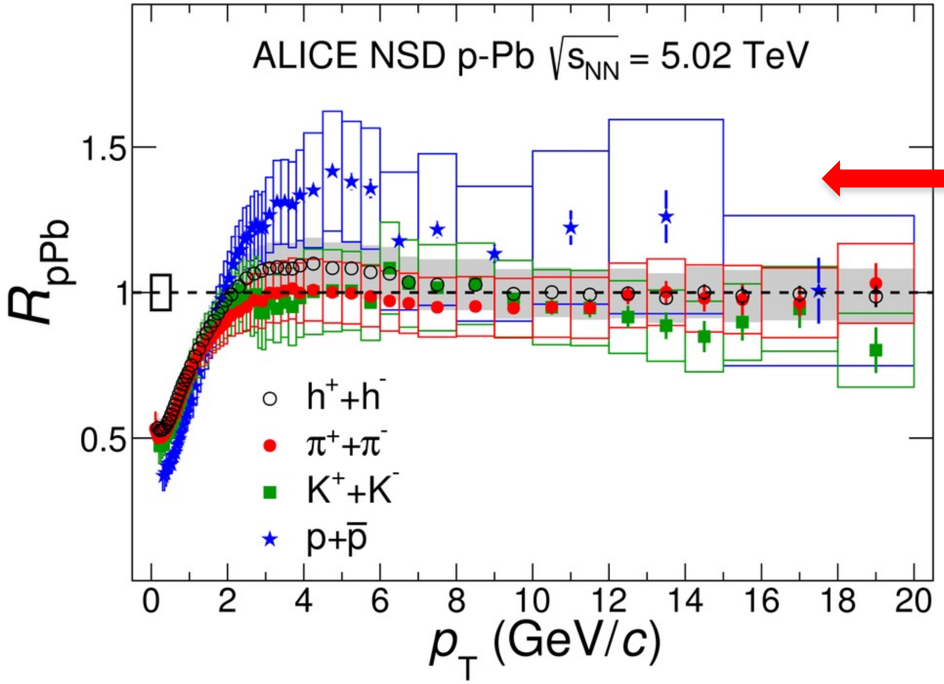

$$R_{\mathrm{pPb}} = \frac{\mathrm{d}^2 N_{\mathrm{pPb}}/\mathrm{d}y\mathrm{d}p_{\mathrm{T}}}{\langle T_{\mathrm{pPb}}\rangle \mathrm{d}^2\sigma_{\mathrm{pp}}^{\mathrm{INEL}}/\mathrm{d}y\mathrm{d}p_{\mathrm{T}}}$$

- Protons show peak at intermediate p_T
- R_{pPb} of π and K not show peak and flat above 2 GeV/c
- mass ordering in the Cronin peak, strong enhancement of protons
- no suppression at high p_T (> 8-10 GeV/c)

Charged hadrons spectra: Pb-Pb 5.02 ATeV

PHYSICAL REVIEW C 101, 044907 (2020)

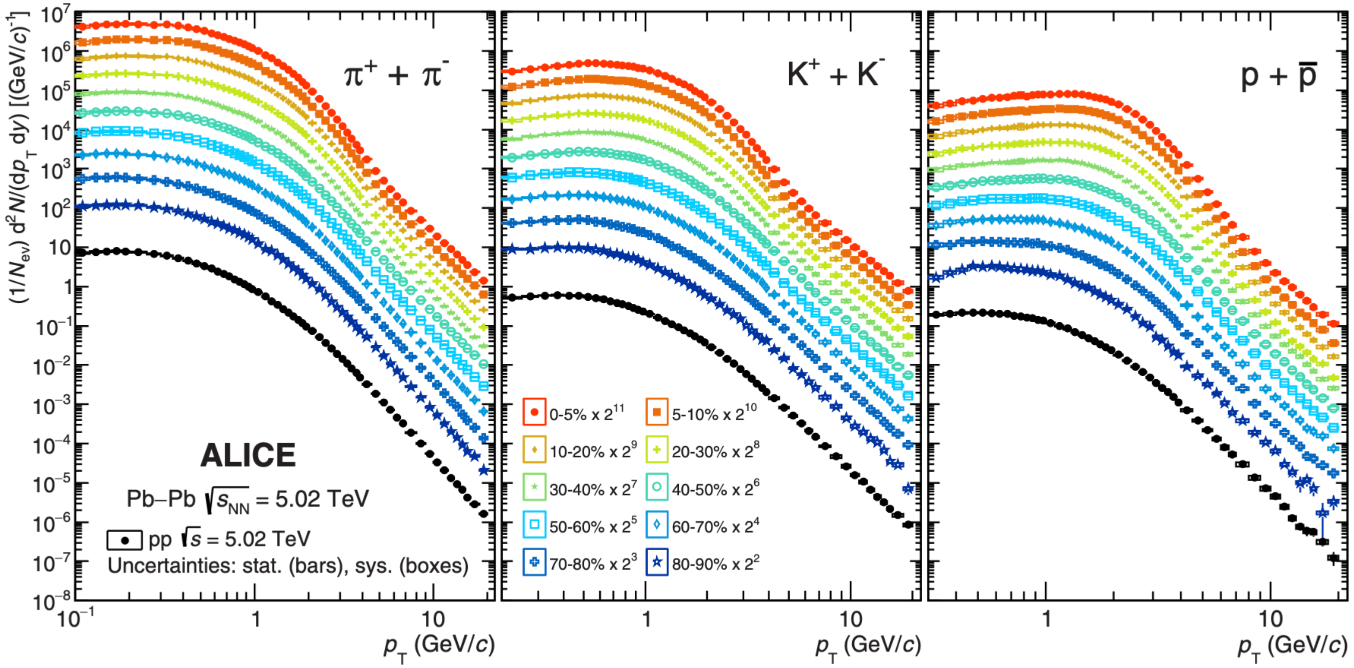

PHYSICAL REVIEW C 101, 044907 (2020)

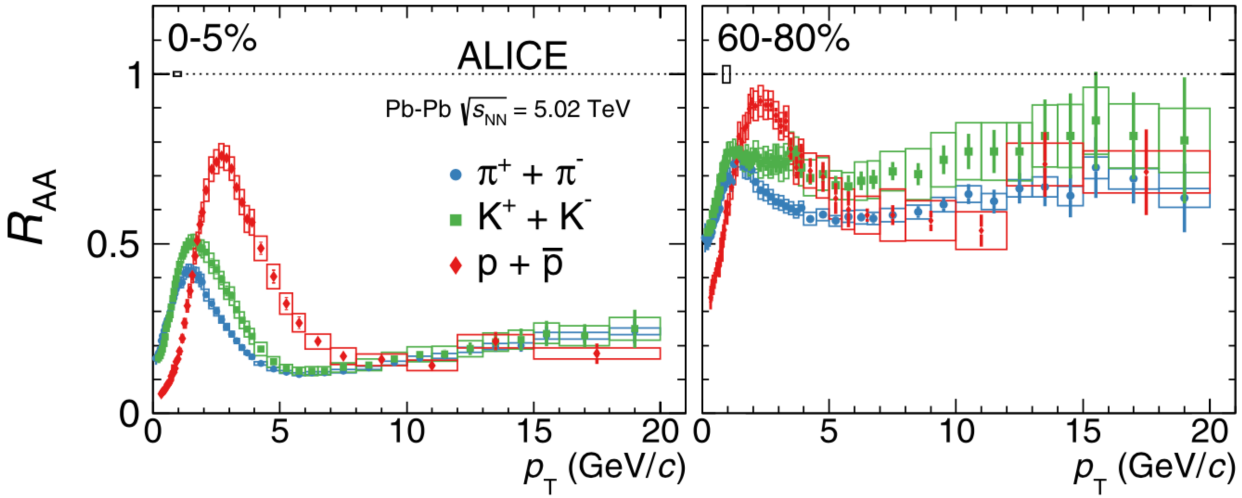

$$R_{AA} = \frac{d^2N_{\text{id}}^{AA}/dy\,dp_T}{\langle T_{AA}\rangle d^2\sigma_{\text{id}}^{\text{pp}}/dy\,dp_T}$$

Deuteron identification: Pb-Pb 2.76 ATeV

Deuterons yield is not enough to allow measurements in HMPID but in central (0-10%) Pb-Pb collisions, by means of statistical unfolding on the mass distribution (not on Cherenkov angle one!)

$$m^2 = p^2(n^2\cos^2\theta_{ckov} - 1)$$

n = refractive index

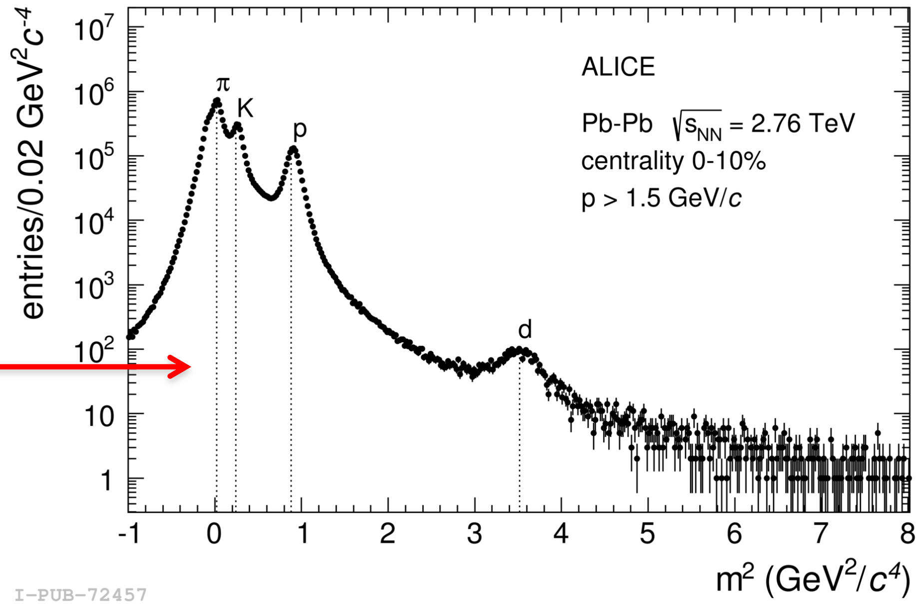

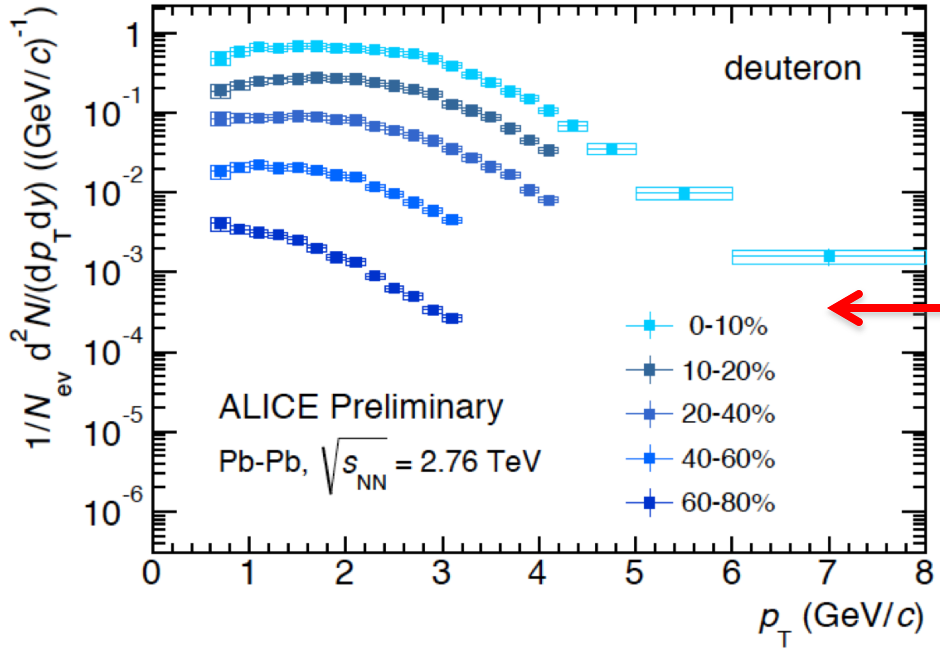

I-PUB-72457

Deuteron spectra in Pb-Pb collisions at $\sqrt{s_{NN}}$ = 2.76 TeV

Deuteron identification: Pb-Pb 2.76 ATeV

Deuterons yield is not enough to allow measurements in HMPID but in central (0-10%) Pb-Pb collisions, by means of statistical unfolding on the mass distribution (not on Cherenkov angle one!)

$$m^2 = p^2(n^2\cos^2\theta_{ckov} - 1)$$

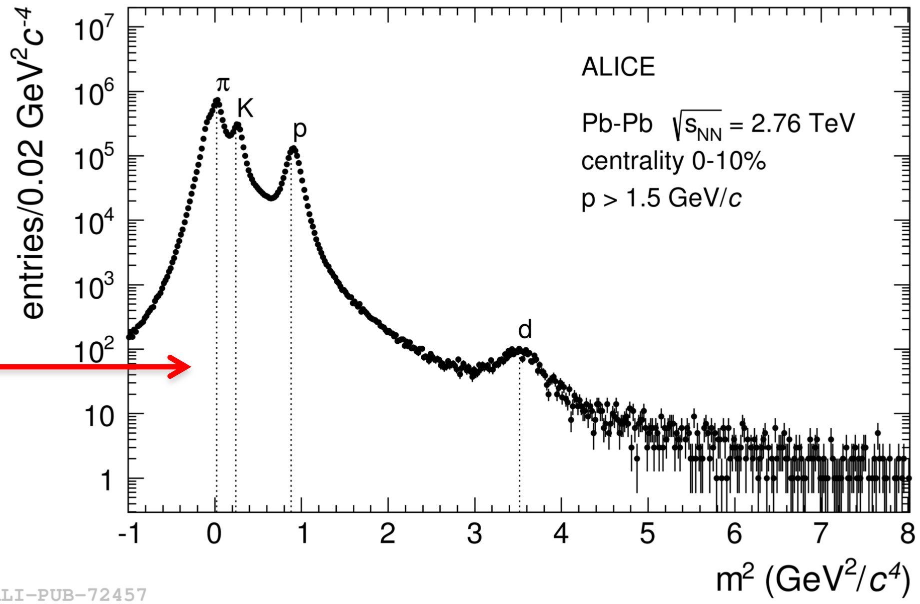

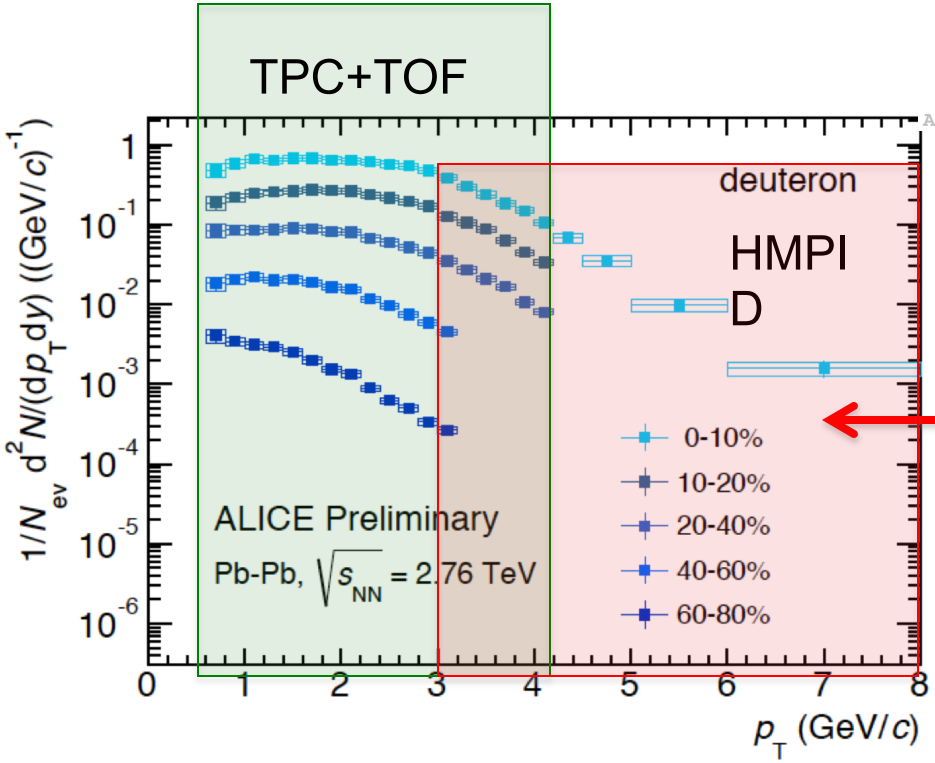

Deuteron spectra in Pb-Pb collisions at $\sqrt{s_{NN}}$ = 2.76 TeV

Good matching with TPC+TOF measurements!

Inclusive hadrons spectra: pp 2.76 TeV

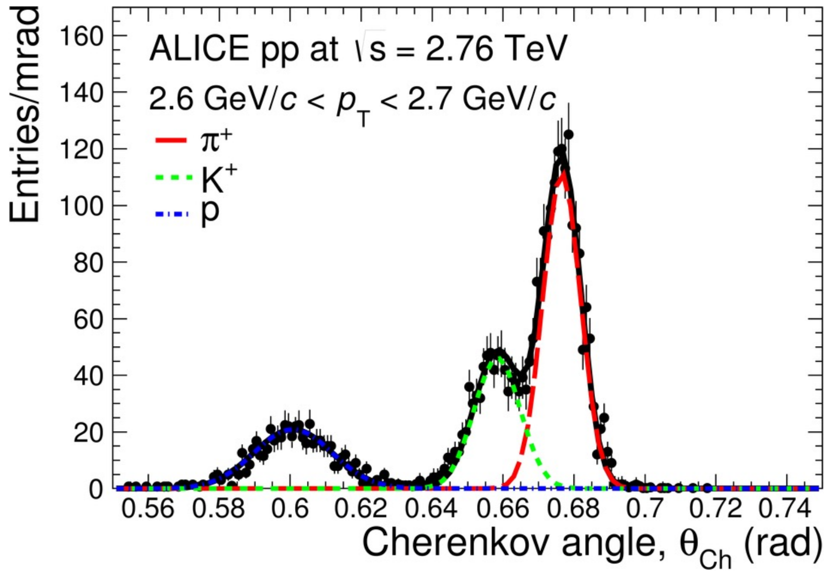

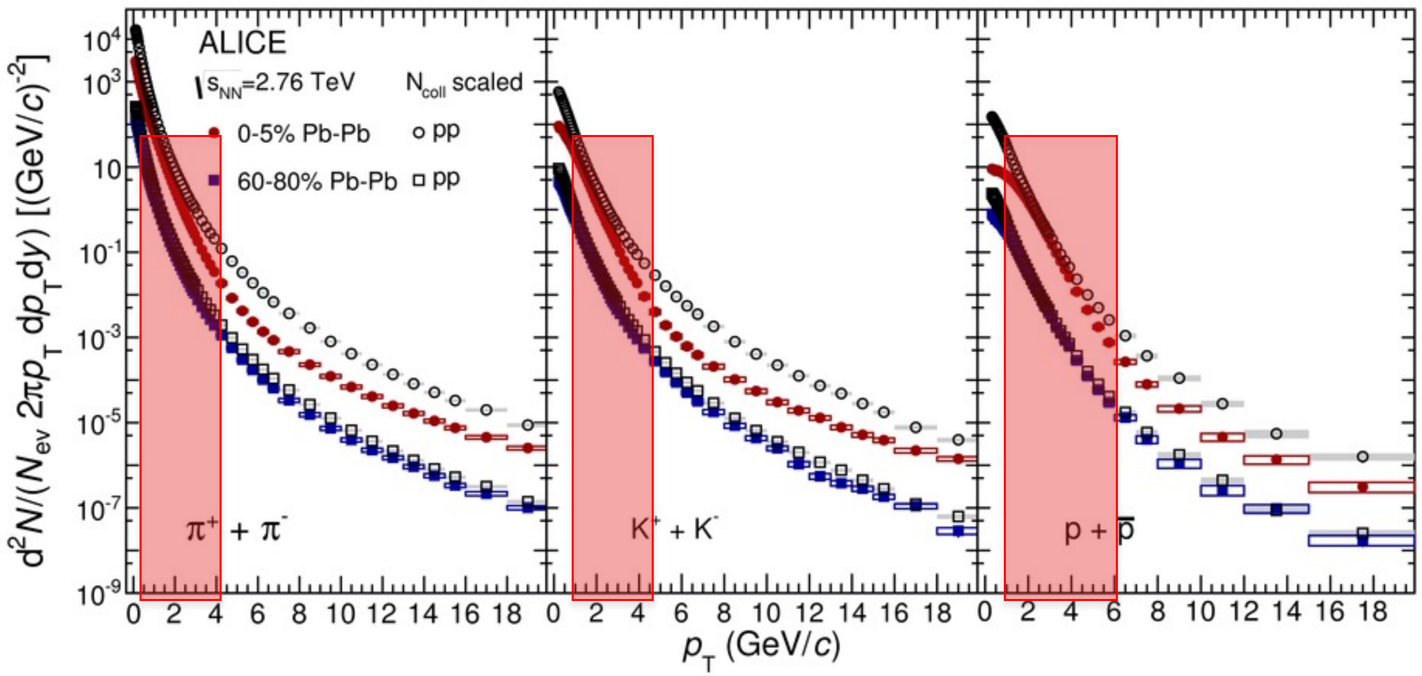

Charged particle PID in ALICE (central barrel)

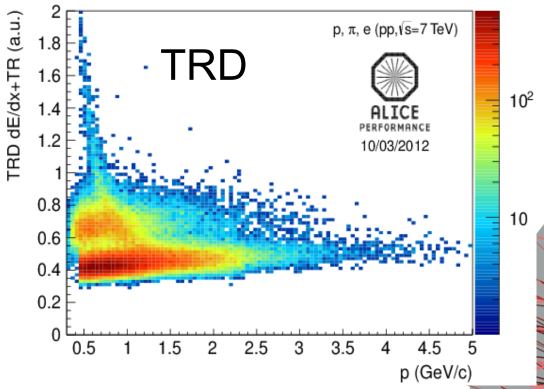

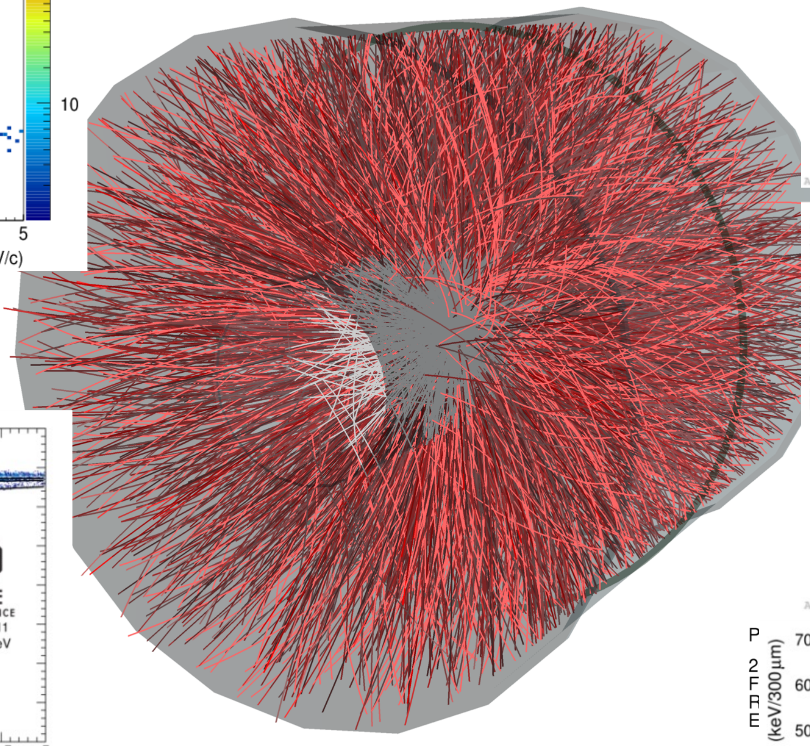

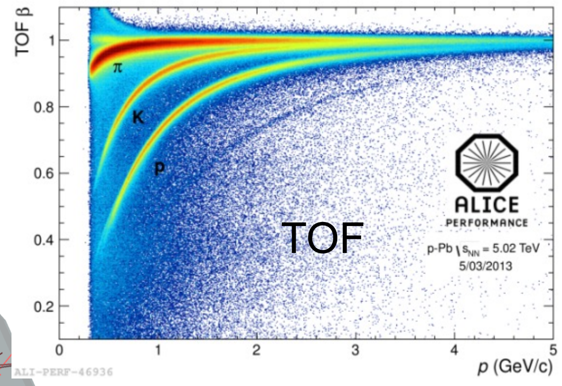

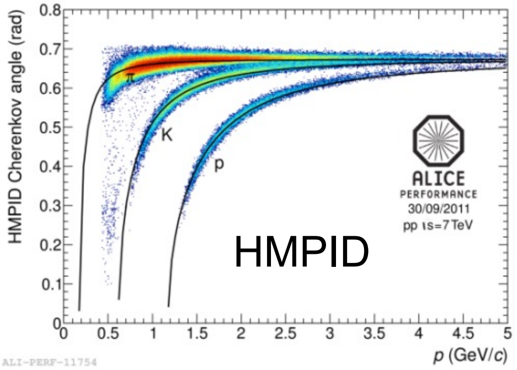

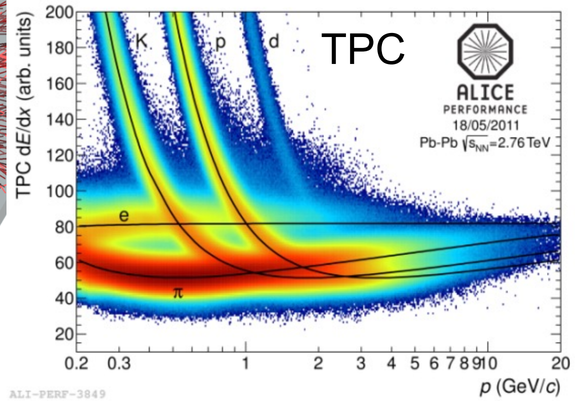

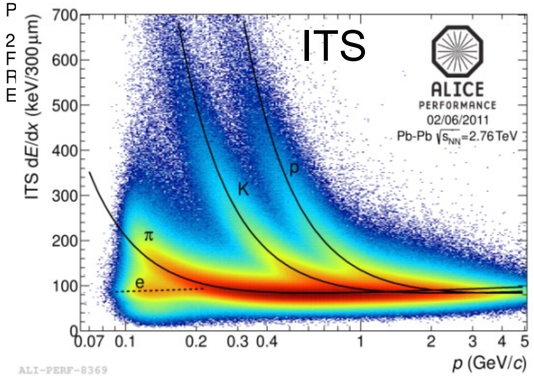

The ALICE experiment is optimized for charged particle tracking **<u>and hadron identification</u>** for $|\eta|<0.8$